الجمـــهوريـــة الجـــزائريـــة الديـمقراطيـــــــة الشـــعبيـــــة
PEOPLE'S DEMOCRATIC REPUBLIC OF ALGERIA
وزارة التعـلـيـم الـعـالـــي والـبـحـث الـعـلـمي
MINISTRY OF HIGHER EDUCATION AND SCIENTIFIC RESEARCH
جـامـعـة عمّـــار ثـلـيـــجـــي بالأغـــواط
UNIVERSITY AMAR TELIDJI LAGHOUAT
كـلـيـــــة الـعـلـــــوم
FACULTY OF SCIENCES
قسم عـلـــــوم المادة
Department OF Material Sciences

Master thesis

Field : Physics

Option : Applied Physics

By:

BEGAGRA Anfal

THEME

Theoretical study on YH_6 cubic system Based on ab initio methods

Defended in 22/09/2020 in front of jury composed of:

Mr. LAGOUN Brahim	*M.C.A*	*President*
Mr. KHENCHOUL Salah	*M.C.A*	*Supervisor*
Mrs. AISSOUS Basma	*M.A.A*	*Examiner*

University year 2019-2020

Dedication

To my first command…

To whom i ask him for a star that will bring me heaven!

To my hero, for everything you did for me…

To you **BEGAGRA.B.H** my father, my boss, my companion and my everything

You never let me down, you never made me frown…

I've only seen happiness with you around…

By making me feel like a princess crowned …

Today I give you my words, my graduation, I had a wish that you'll be present…

To her who gave me a life, the symbol of tenderness…

Who sacrificed herself for my happiness and success…

Today I dedicate you **Mom**, thank you for all years you dedicated for me.

I love you

To my **grand-parents**

To my sisters: **NourElhouda, Issraa, Yassmine**

To my brothers: **Yassine and Abdessamad**

To you my soul mates and my best friends

B.Soumia, K.Fatiha, K.Maria, H.Hanane, C.F.Zohra, A.Hanane

Thanks for been around all time and full of love and friendship

Thanks for every person passed in my life and left a beautiful touch

With regard to the thanks, which are of a special kind

wewill direct it to all those have stopped on our

path or tried to stop us from walking. We would tell you

that if you weren't here, we wouldn't have felt the pleasure of looking.

B.ANFAL

Acknowlegment

الحمد لله الذي هدانا لهذا و ما كنا لنهتدي لولا أن هدانا الله

First of all I warmly want to thank **Amar Thlidji University** at **Laghouat**

It is very difficult for me to express in these few lines

All my gratitude appreciation

To my supervisor **Mr.KHENCHOUL Salah** who told me that

The success is special kind of happiness.

To have proposed and directed this work

But above all to have spared his time to put at my disposal

All the necessary means.

I am very grateful to him for his help, his advices, his skills, but also for

His good humor and his modest high.

I sincerely thank **Mr.LAGOUN Brahim** who did me

The honor of presiding over my jury.

For his constant support and advices, which I benefited from.

I also thank the jury member **Mrs.AISSOUS Basma**

For agreeing to review this work and to enrich it with her proposals.

Table of contents

List of figures

List of tables

List of abbreviation

BCS	Baredeen, Cooper and Schreiffer
Tc	Critical temperature
Bc	Critical magnetic field
Ic	Critical electric current
MRI	Magnetic resonance imaging
MAGLEV	Magneticly levitated
DFT	Density functional theory
DOS	Density of state
LDA	Local density approximation
GGA-PBE	Generalized gradient approximation in the Perdew-Burke-Ernzerhof
ZB	Brilloin zone
TDOS	Total density of state
PDOS	Partial density of state
PP	Pseu Potential
PW	Plane wave
SCF	Self consistent field
DFPT	Density functional perturbation theory

General introduction

General introduction:

Superconductivity is the ability of material to conduct electricity without any resistance, the first observation was in 1911 by K.Onnes in solid mercury that presented two important propreties below certain temperature which are perfect electricity conduction and magnetic flux expulsion that is called Meissner effect [1, 2].

The first successful theory to explain the microscopic mechanism of superconductivity in metals and alloys was proposed by Bardeen, Cooper and Schrieffer in 1957 called BCS theory [3]. Ever since, countless scientists have been searching for a material whose Tc exceeds room-temperature, the discovery of high temperature superconductivity in cooper oxides raised Tc above liquid Helium temperature. Since 1994, one of the cooper oxides has held the record for the highest Tc (133 K° at atmospheric pressure and 164 K° under high pressure) [4].

Ashcroft predicted that certain Hydrogen-rich solids might become metallic at lower pressures than elemental Hydrogen and they would possess the same propreties conductive to high temperature superconductivity in compressed hydrides solids containing Hydrogen atoms bonded to other elements. Two properties of metallic hydrides are particularlybeneficial for promoting high Tc superconductivity: the first is alarge H-derived electronic density of states at the Fermi level, and the second is large modifications of the electronic structure inresponse to the motion of the H atoms (electron-phononcoupling). It appears to be important to satisfy both of thesecriteria in hydrides with high H content in order to achieve high Tc values [5, 6].

Understanding the physics of a superconducting material requires the knowledge of its structure, phase stability, structural propreties, and critical parameters (critical temperature, critical magnetic field and critical current) to define the superconductive area, due to simulation methods these propreties could be determined; indeed, they have given a new dimension to the scientific investigation of many physical and chemical phenomena. These techniques may have replaced the experimental part, specificallywhen the experience is expensive, dangerous or unattainable in the laboratory. The ab initio methods allow to give an estimation of measurable physical quantities comparable to the experience based on quantum mechanics principals giving the most possible exact energy calculations of N particles system from electronic structure of each constructive elementby resolving Schrödinger equation.

The goal of this thesis to attain more understanding the structural and vibrational propreties under high pressures, superconducting gap, critical parameters of cI14-YH_6phase as Tc and Bc by using the ab initio calculations in the framework of density functional theory (DFT) employing ABINIT software [7].

The thesis is composed of three chapters. In the first chapter, the phenomenon of superconductivity is introduced in a general way andHigh pressure effect on superconductivity. The second chapter contains the theoretical foundations of density functional theory (DFT), which is one of the ab-initio methods for predicting the properties of materials. The third chapter presents the results of our calculations with a parallel discussion and a comparison of these with the results of other and theoretical works.

References

[1] H. KamerlinghOnnes. Commun. Phys. Lab. Univ. Leiden. Suppl., (1911).

[2] W. Meissner and R. Ochsenfeld. Naturwiss, 21 : 787–788, (1933).

[3] J. J. Bardeen, L. N. Cooper, and J. R. Schrieffer. Phys. Rev. 108 : 1175, (1957).

[4] A. P. Drozdov, M. I. Eremets, I. A. Troyan, V. Ksenofontov, andS. I. Shylin, Nature 525, 73(2015).

[5] N. W. Ashcroft, Phys. Rev. Lett. 21, 1748 (1968).

[6] N. W. Ashcroft, Phys. Rev. Lett. 92, 187002(2004).

[7] X. Gonze, et al, Z. Kristallogr. 220, 558, (2005).

Chapter I : Superconductivity

I.1. Introduction

Superconductivity is the set of physical properties experiential in some materials where electrical resistance vanishes and magnetic flux fields are excluded from the bulk of the material below set temperature. Any material exhibiting these properties is a superconductor. Unlike an ordinary metallic conductor, whose resistance decreases gradually as its temperature is lowered even down to near absolute zero, a superconductor has a characteristic critical temperature below which the resistance drops abruptly to zero. An electric current through a loop of superconducting wire can persist indefinitely with no power source.

In this Chapter, we will display the most important milestones that the development of these materials has gone through. Over this part, we will learn about the aspirations of researchers and industrialists in this field.

I.2. Brief history

The first observation was in 1911 by Dutch physicist Heike Kamerlingh Onnes who was studying the resistance of solid mercury at cryogenic temperatures using the recently produced liquid helium as a refrigerant. At the temperature of 4.2 K, he observed that the resistance abruptly disappeared [1]. In the same experiment, he also observed the superfluid transition of helium at 2.2 K, without recognizing its significance. The precise date and circumstances of the discovery were only reconstructed a century later, when Onnes's notebook was found. In subsequent decades, superconductivity was observed in several other materials. In 1913, lead was found to superconduct at 7 K, and in 1941 niobium nitride was found to superconduct at 16 K [2].

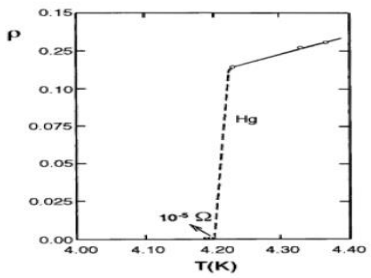

Fig I.1: Illustration of Kamerlingh Onnes's discovery of superconductivity and vanishing of the electrical resistivity [1].

Chapter I

Superconductivity

In 1933, W. Meissner and R. Ochsenfeld [3] observed that under a specific temperature value the magnetic field is expulsed from the interior of a material that is in the process of becoming a superconductor. The first successful set of phenomenological equations for superconducting metals, were given by F. London in 1935 [4]. In 1950 almost 40 years after the discovery of the phenomenon, there was no any adequate microscopic theory of superconductivity. However, by 1935, single elements necessary to a successful theory to explain superconductivity was known to theorists. The peculiar of condensation of Bose-Einstein gas was predicted by Einstein in 1925 [5,6]. The idea is that pairs of fermions can be combined to form bosons has been known since 1931. In 1950 the most relevant ideas of superconductivity have been summarized by F. London in his famous book “superfluids” [7]. At last, Bardeen, Cooper and Schrieffer (BCS) theory (1957) [8], was the first successful theory to explain the mechanism of superconductivity in metals and alloys.

In 1968, Neil Ashcroft [9] predicted that metallic Hydrogen should have all the propreties required to be a High-Temperature superconductor according to BCS theory. Unfortunately, metallizing Hydrogen in static compression experiments turned out to be extremely difficult. Ashcroft further predicted that certain Hydrogen rich solids might become metallic at lower pressures than elemental Hydrogen and that they would possess the same propreties conductive to High-Temperature superconductivity. This hypothesis catalyzed the search for superconductivity in compressed hydrides solids containing Hydrogen atoms bonded to other elements.

In 1986, more than 70 years after the discovery of superconductivity, J. G. Bednorz and K. A. Müller [10] put this phenomenon back at the heart of scientific news by highlighting the superconductivity in a barium-lanthanum-copper oxide at the surprisingly high temperature of 35 K. A new family of superconductors has just been born. Shortly after this scientific tornado, other compounds of the same family emerge with increasingly hot critical temperatures over time. The temperature record today is 133K in $HgBa_2Ca_2Cu_3O_x$. These compounds all have different structures but have in common the “active” CuO_2 planes within which superconductivity is formed. One main objection to the BCS theory as applied to these materials is that this theory is founded on the notion of the Landau quasiparticles, which in these superconductors, especially in the under-doped region, are not well-defined. In other words, the starting point of the BCS theory is a mean-field theory for the electronic degrees of freedom; coupling these mean-field electrons to bosonic excitations (such as phonons, as pointed out by C. Binek here above, but not exclusively [11]), one can arrive at a

superconducting state, depending on the physical conditions (such as temperature). In high-T_c superconductors this hierarchical separation of the degrees of freedom does not apply.

In 2004, Ashcroft [12] predicted that certain Hydrogen-rich might become metallic at lower pressures than elemental Hydrogen and that would possess the same propreties conductive to High-temperature superconductivity. This hypothesis catalyzed the search for superconductivity in compressed solid hydrides containing Hydrogen atoms bonded to other elements. To study superconductivity in these compressed materials, researchers need to carry out static High-pressure experiments in which the materials are squeezed in Diamond Anvil Cells (DAC). Such experiments are expensive, technically challenging and can be difficult to interpret. What's more, the material phases that are stable under pressure can be different than the ones we know to occur at atmospheric conditions. As result, quantum mechanics based computations have become extremely important in guiding these experiments, in particular by pinpointing promising compounds.

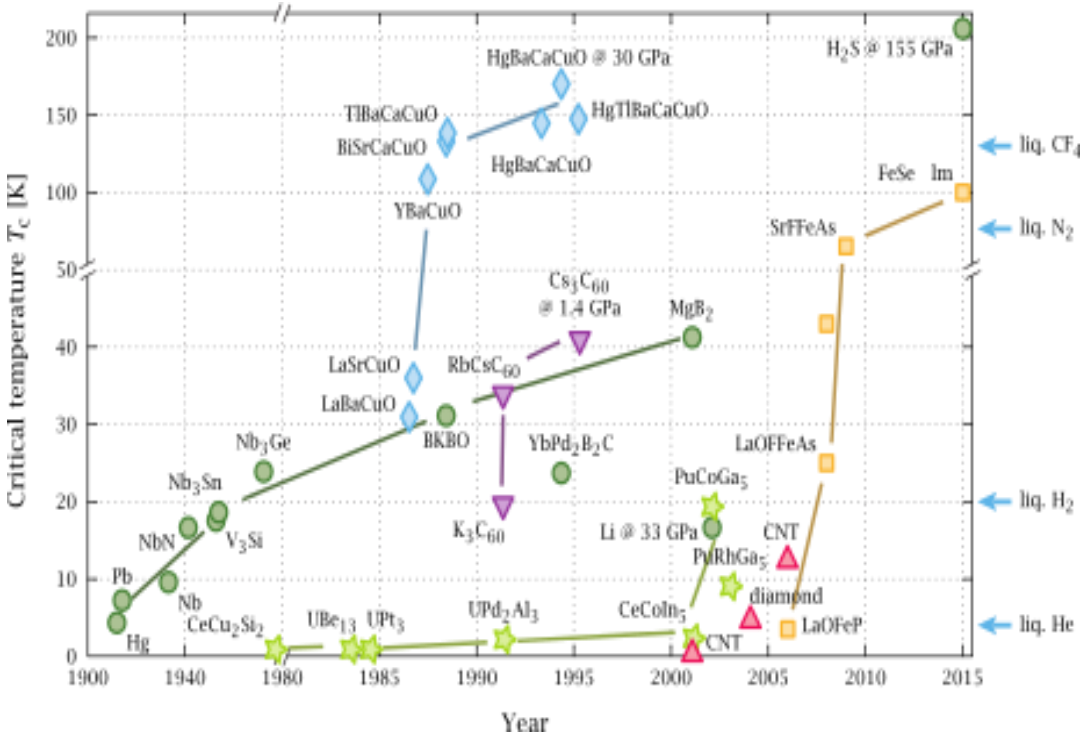

Fig I.2: Survey diagram for superconductors [13].

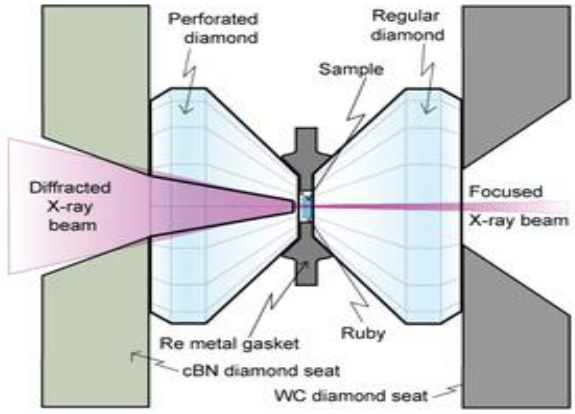

Fig I.3: Diamond Anvil Cell [14].

Table I.1: Examples of previous calculations of superconducting hydrides at high pressure P [15]

Hydride (P GPa)	max T_c (K)	Hydride (P GPa)	max T_c (K)	Hydride (P GPa)	max T_c (K)
H solid (500)	217	HfH_2 (260)	13	AlH_5 (250)	146
LiH_6 (150)	38	VH_8 (200)	71.4	GaH_3 (160)	86
KH_6 (166)	70	NbH_4 (300)	38	InH_3 (200)	40
BeH_2 (400)	62	TaH_6 (50)	120	$Si2H_6$ (362)	79
MgH_6 (300)	260	CrH_3 (81)	37.1	GeH_8 (250)	90
CaH_6 (150)	235	TcH_2 (200)	11	SnH_4 (200)	62
BaH_6 (100)	38	FeH_5 (150)	52	PbH_8 (230)	107
ScH_6 (285)	130	RuH_3 (100)	3.6	PH_3 (207)	103
YH_{10} (300)	323	OsH (100)	2.1	AsH_8 (350)	151

I.3. Superconducting materials propreties:

I.3.1. The zero resistance

In a superconductor, below a temperature called the critical temperature, the electric resistance very suddenly falls to zero. At zero resistance the material conducts current perfectly. This is incomprehensible because the flaws and vibrations of the atoms should cause resistance in the material when the electrons flow through it. However, in a superconductor, the electric resistance is equal to zero although the flaws and vibrations still exist. Even though the current is perpetual, it is not a violation of the thermodynamic lows. The electrons form a new original quantum collective state that is not sensitive to collisions anymore. The electrons are not slowed, and the electric resistance has disappeared.

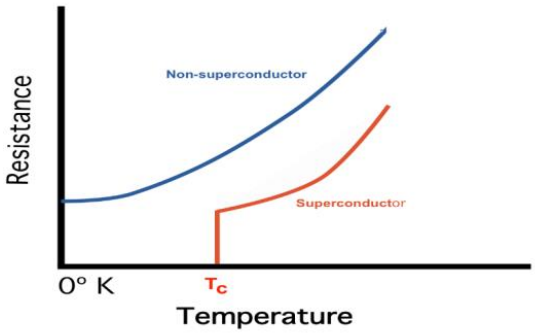

Fig I.4: The phase transition between the normal conductor phase and superconductor phase.

I.3.2. The Meissner effect:

The Meissner effect [3] is a phenomenon that occurs in superconductors below the critical temperature which is where a superconductor expels all magnetic field from within itself. One of the most well-known demonstration of Meissner effect is its ability to make a magnet levitate above a superconductor.

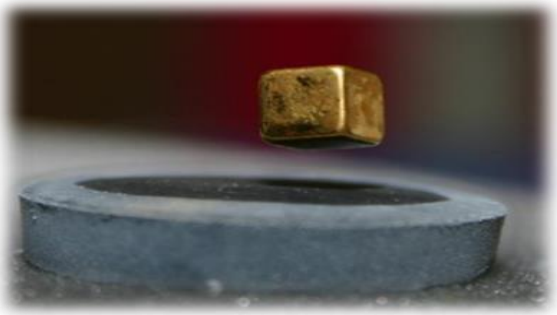

Fig I.5: A magnet is able to levitate above a superconductor due to Meissner effect [16].

When a superconductor is below the T_c, the applied magnetic field is expelled from the interior of the superconductor and bent around it. These magnetic fields are expelled because of under influence of a magnetic field, surface current that flows without resistance develop to create a magnetization within the superconductor. This magnetization is equal and opposite of the magnetic field, resulting in cancelling out the magnetic field everywhere within the superconductor.

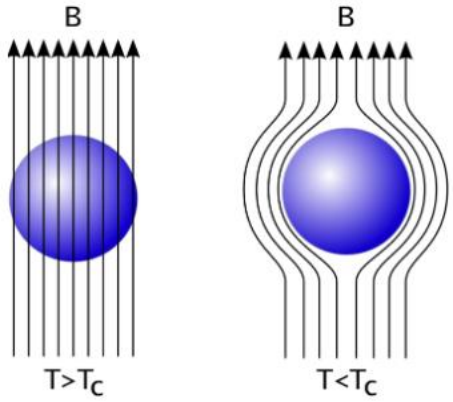

Fig I.6: A comparison between how a superconductor acts when it is above and below the Tc.

Above the critical temperature, the magnetic field is allowed to pass through the superconductor. But when the superconductor is below the critical temperature, the magnetic field lines are bent around it.

I.4. Different types of the superconductors:

While superconductors may appear to react the same when in an applied magnetic field, there are differences that separate superconductors into two categories depending on how they react. For all superconductors, there is a maximum magnetic field, called the critical magnetic field B_c that can be applied before magnetization opposing the magnetic field reaches a maximum and the superconductor revert to its non-superconducting state [17, 18].

I.4.1. Type I superconductors:

For a Type I superconductor, the direct relationship between the applied magnetic field and the opposing magnetization follows until the critical magnetic field is reached and the super-conduction no longer occurs. When this point is reached, the Meissner effect vanishes and the magnetic field is able to pass through the superconductor unhindered.

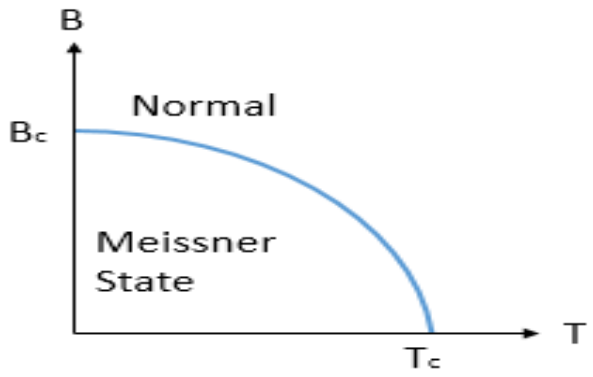

Fig I.7: The range of the Meissner effect for a Type I superconductor.

I.4.2. Type II superconductors:

For Type II superconductors, there is an additional state that occurs between the Meissner state and the normal state. This state called the mixed state or the Vortex state, is noted by the mixing of the normal and Meissner state. The magnetic field is allowed to pass through the superconductor at specific parts where the normal state is occurring, while the rest of the superconductor exhibits the Meissner effect and expels the magnetic field. The shift from the Meissner effect to the Vortex state occurs at lower critical magnetic field Bc_1. This Vortex state continues to occur to the upper critical magnetic field Bc_2, where the magnetic field becomes so strong for the superconductor to expel and

the superconductor allows all magnetic fields to pass through it, returning it to its normal state. Between these two extremes the Vortex state occurs, where small tubular regions develop in the superconductor inside which the superconductor is in the normal state. Through these flux tubes or vortices, the magnetic field is allowed to pass. As with the edge of the superconductor, currents develop on the inside of the flux tubes, preventing the magnetic field from passing into the Meissner state sections of the superconductor. It is within this vortex state that flux pinning occurs.

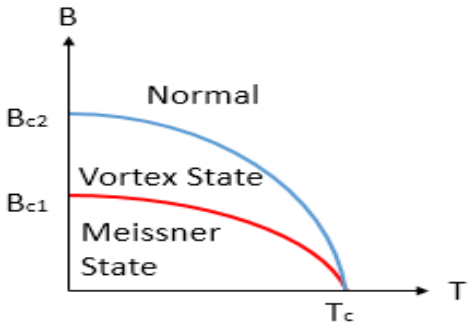

Fig I.8: The range of the different states for a Type II superconducting.

The upper limits at the critical superconductor, with the Meissner state ranging from temperature Tc, and the critical magnetic field Bc. zero to the lower critical magnetic field, Bc_1, and the Vortex state ranging from the lower critical magnetic field to the upper critical magnetic field Bc_2

I.5. Critical parameters:

I.5.1. The critical temperature:

The critical temperature of superconductors is the temperature at which the electrical resistance of a metal drops to zero. The transition is so sudden and complete that it appears to be a transition to a different phase of matter.

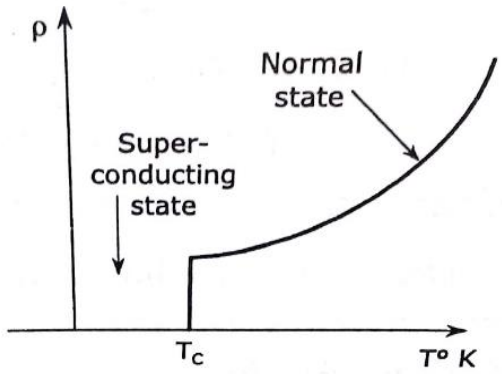

Fig I.9: Variation of the resistivity with temperature of superconductor.

I.5.2. Critical magnetic field:

The superconducting state cannot exist in the presence of a magnetic field greater than a critical value even at absolute zero. This critical magnetic field is strongly correlated with critical temperature of the superconductor, which is in turn correlated band-gap. Type II superconductors show two critical magnetic field values, one at the set of mixed superconducting and normal state and the other where superconductivity vanishes. It is the nature of superconductors to exclude magnetic fields (Meissner effect) so long as the applied field does not exceed their critical magnetic field. This critical magnetic field id tabulated for 0 K° and decreases from that magnitude with increasing temperature, reaching zero at the critical temperature of superconductivity. The critical magnetic field at any temperature below the T_c is given by the empirical relationship:

$$B_C(T) \approx B_C(0)\left[1 - \left(\frac{T}{T_C}\right)^2\right] \qquad \text{(I.1)}$$

I.5.3. Critical current:

When the current passes through the superconductor exceeds a certain critical value the superconducting propriety will be destroyed. The current density related to the critical magnetic field is called critical current I_c.

$$I_c = 2.\pi.r.B_c/\mu_0 \qquad \text{(I.2)}$$

It means the minimum current in the material without destroying the superconductivity.

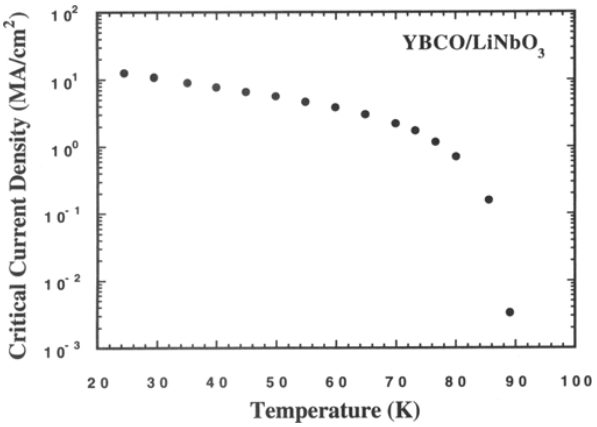

Fig I.10: Critical current density measurement of YBa2Cu3O7 cuprate with temperature [19].

I.6. Electron-Phonon interaction:

The Electron-Phonon interaction is the source of the attraction that binds two electrons into a paired state, generally referred to as Cooper pairs. The ions within the lattice are oscillating about their equilibrium positions due to thermal energy. The resulting propagating lattice vibrations are called phonons, as they are essentially sound waves. The electrons then interact with the ions as they move through the lattice - causing charge distortions that propagate along the lattice structure, in turn causing distortions in the periodic potential. These distortions can affect the motion of another electron at some distance that is also interacting with the lattice in a similar way - this is thus called an *electron-phonon interaction*, and is an integral part of Cooper pair formation.

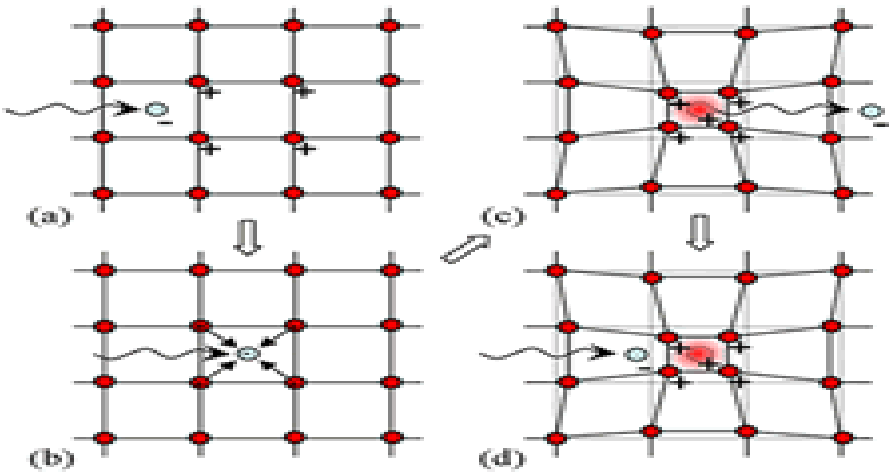

Fig I.11: Mechanism of the electron-Phonon coupling.

I.7. Bardeen-Schrieffer-Cooper (BCS) theory:

For many years, the phenomenon of superconductivity could not be satisfactorily explained by the laws of conventional physics. In 1950, American physicists John Bardeen, Leon Cooper, and John Schrieffer formulated a theory for superconductivity that earned them the Nobel Prize in physics in 1972 [8]. According to the BCS theory, electrons are able to travel through a solid with zero resistance because of attractive interactions involving two electrons that are at some distance from each other. As one electron moves through the lattice, the surrounding nuclei are attracted to it. The motion of the nuclei can create a transient (short-lived) hole that pulls the second electron in the same direction as the first. The nuclei then return to their original positions to avoid colliding with the second electron as it approaches. The pairs of electrons called Cooper pairs, migrate through the crystal as a unit. The electrons in Cooper pairs change partners frequently, like dancers in a ballet. According to the BCS theory, as the temperature of the solid increases, the vibrations of the atoms in the lattice increase continuously, until eventually the electrons cannot avoid colliding with them. The collisions result in the loss of superconductivity at higher temperatures.

An important parameter which characterizes Cooper pair is coherence length ξ_0 (the size of the Cooper pair).

$$\xi_0 = \frac{2\hbar v_F}{\pi \Delta_0} \tag{I.3}$$

ħ is Planck constant, v_F is the electrons velocity at Fermi level and Δ is the superconducting gap. For elemental superconductors the characteristic length of Cooper pair is about 10^{-7} m. Distance between ions in the lattice is about 10^{-10} m. between two paired electrons there are thousands of other free electrons which don't influence on this interaction.

The size of the energy gap depends on temperature and can be described as follows:

$$\Delta(T) = \Delta_0 \left(1 - \frac{T}{T_c}\right)^{1/2} = 1.76 k_B T_c \left(1 - \frac{T}{T_c}\right)^{1/2} \tag{I.4}$$

Where $\Delta_0 = 1.76 k_B Tc$ is the superconducting gap at T=0 K and k_B is the Boltzmann constant.

Description of BCS theory was made in the assumption of weak electron-phonon coupling and gives Tc as:

$$T_c = 1.14\left(\frac{\hbar\omega_D}{k_B}\right) exp\left(-\frac{1}{N(E_F)V_{eff}}\right) \quad (I.5)$$

Where ω_D is the Debye frequency, $N(E_F)$ is the density of state at Fermi level and V_{eff} is net potential between electrons.

I.7.1. Eliashberg theory:

In 1960 Eliashberg developed a generalized theory of superconductivity. He took into account retardation – the second electron interacts with the polarized lattice, and this polarization takes a time – it is quick for light atoms and slow for heavy atoms. Coupling constant λ represents the strength of electron-phonon interaction and can be calculated:

$$\lambda = 2\int_0^\infty \frac{\alpha^2 F(\omega)}{\omega} d\omega \quad (I.6)$$

(ω) is the phonon density of states and the pairing function $\alpha^2(\omega)$ is defined:

$$\alpha^2 F(\omega) = \frac{1}{\rho_0}\sum_{kk'}|g_{kk'}|^2 \rho^{ph}_{k-k'}(\omega)\delta(\mu - \varepsilon_k)\delta(\mu - \varepsilon_{k'}) \quad (I.7)$$

In terms of the electron-phonon coupling constants $g_{kk'}$ and the phonon spectral function ρ_{ph} for the wave vector k. Here, ε_k is the energy of an electronic state with the wave vector k and μ is the chemical potential. If the spectral function ρ_{ph} q(ω) is replaced by results for non-interacting phonons. The effective λ is typically larger than the bare λ_0, due to a renormalization of (ω) and the effective phonon frequency ω_0^r. $\lambda \ll 1$ corresponds to weak electron-phonon interactions, $\lambda \sim 1$ corresponds to intermediate electron-phonon interactions and $\lambda > 1$ corresponds to strong electron-phonon interactions.

An analytical and numerical solution of Eliashberg theory was made by McMillan and re-examined by the Allen-Dynes. Generalized equation for Tc is:

$$T_c = \frac{\theta_D}{1.45} exp\left[\frac{-1.04(1+\lambda)}{\lambda - \mu^*(1+0.62\lambda)}\right] \quad (I.8)$$

Where $\langle\boldsymbol{\omega}\rangle$ is the weighted average over the phonon frequency spectra and μ^* is the Coulomb pseudopotential which takes into account the Coulomb repulsion between the electrons [20].

I.8. High Pressure effects on superconductivity:

The presence of the superconductivity in the specific material is determined by its phonon and electronic structure. Changing of temperature of material leads to changing in the occupation of energy levels. Pressure changing leads to modification of energy levels and electronic configuration. Eliashberg theory and McMillan expression for T_c can only tell us that dependence of T_c on pressure is very complicated and can be different for different materials [20, 21]. If we assume that Coulomb pseudopotential doesn't depend on pressure than from Eliashberg formulation we can get:

$$\frac{d\ln T_c}{dp} = \frac{1}{B}\left\{\gamma + \left[\frac{1.04\lambda}{\lambda-\mu^*(1+0.62\lambda)} - \frac{1.04\lambda(1+\lambda)(1-0.62\mu^*)}{[\lambda-\mu^*(1+0.62\lambda)]^2}\right]\left[2\gamma + \frac{d\ln\eta}{d\ln V}\right]\right\} \quad \text{(I.9)}$$

Where B is the bulk modulus, $\gamma = -\mathrm{d}\ln\langle\omega\rangle/d\ln V$ is the Grüneisen parameter and $\eta = (Ef)\langle I^2\rangle$, and $\langle I^2\rangle$ is the average squared electronic matrix element.

Experimental studies show that for most elemental *s*, *p* metals, the T_c most often decrease with pressure increasing. Transition metals have *d* character superconductivity and electronic structure of these metals is more complicated. Complexity of electronic structure leads to different response of T_c on pressure increase. For some transition metals T_c increases with pressure increasing, for some decreases. For the non-metal material increase of the pressure can lead to transformation to metal and paring of superconductivity [21].

I.9. Application

Superconductivity has been an exciting field for engineers over the years. They've used superconductivity in magnets to make ultra-strong magnets needed in MRI machines. They have used superconductive magnets in elevated trains (MAGLEV). Superconducting circuits allow for faster computer performance. Innovators at the Jet Propulsion Laboratory have used superconductive magnets to levitate mice in zero gravity experiments. Superconductivity has the potential to allow for very efficient high voltage long distance power transmission. The application of superconductive technology is infinite given we can figure out how to make it cost effective [22].

I.9.1. Magnetic resonance imaging (MRI):

If you set up a current in a loop of superconductor there is nothing to stop it and it will continue flowing forever, forming a very powerful electromagnet, that needs no maintenance other than keeping them cold. The strongest man made permanent magnetic fields are produced using superconductors.

Superconducting magnets are used in MRI (Magnetic Resonance Imaging) which is a way of looking at the soft parts of the body.

I.9.2. Particles accelerators

Superconducting magnets are also going to be used in the new 'Large Hadron Collider' experiment at the CERN Particle Physics Lab. The idea is to accelerate protons and antiprotons to almost the speed of light in a circle and then smash them together. To keep the particles in a circle requires huge magnetic fields which can only be provided by superconductors.

I.9.3. Levitating trains (potential application):

It is also possible to use superconducting magnets to produce a levitating train. The idea is to put very powerful light superconducting magnets on the train, then use copper coils in the track which use repulsion to lift the train up to make it levitate. It is also possible to use the track magnets to push the train along. Because this force is not limited by friction between wheels and a track it is theoretically possible for a maglev train to go much faster and more importantly accelerate and brake faster than a conventional train. Various test maglev trains have been built, in Birmingham, Japan and Germany, although the only one used commercially is a German design built in Shanghai, which uses very strong permanent magnets instead of superconductors [22].

I.9.4. Power cables

An obvious use of superconductors would be to move power around, huge amounts of electrical energy are wasted just heating up power cables, and superconductors would help. However if you put alternating current through them they are no longer lossless, and it reqiures a lot of energy to cool them, so although it is possible they could be used to save energy in the long run in the short

term it is more likely they will be used to save space, superconducting cables have been installed in Chicago and Copenhagen, in old cable ducts with restricted space, allowing you to get more power through the same duct, hence saving lots of money digging up the road. Similarly the US Navy is very interested in them for making small powerful electric motors to power ships with, because it is efficient to put the propellers on pods under the ship however the bigger the motor the more drag it produces, so a much smaller superconducting motor would be advantageous [22].

References

[1] H. Kamerlingh Onnes, *Proc. Sect. Sci*. **13** (1911) 1274–1276.

[2] D. Van Delft & P. Kes, *Physics Today*, **63** (9) (2010) 38–43.

[3] W. Meissner & R. Ochsenfeld, *Naturwissenschaften*, **21** (44) (1933) 787–788.

[4] F. London & H. London, *Proc. Roy. Soc. Lond A*, **149** (866) (1935) 71–88.

[5] S. N. Bose, *Zeitschrift für Physik*. **26** (1) (1924)178–181.

[6] A. Einstein, *Sitzungsberichte der Preussischen Akademie der Wissenschaften*. **1** (1925) 3.

[7] F. London, "Superfluids," Vol. 1, Wiley, New York, (1950).

[8] J. Bardeen, L. N. Cooper, J. R. Schrieffer, *Phys. Rev*, **108** (5) (1957) 1175–1204.

[9] N. W. Ashcroft, *Phys. Rev. Lett*, 21 (1968) 1748.

[10] J. G. Bednorz & K. A. Mueller, *Z. Phys. B*, **64** (2) (1986) 189–193.

[11] D. Pines, *Prog and Prosp*, *Physica* C **282** (1997) 273.

[12] N. W. Ashcroft. *Phys. Rev. Lett*, **92** (2004) 187002.

[13] Superconductor history, Available at: http: //en.wikipedia.org/wiki/File: Sc_history.gif (2011).

[14] Bassett, William A., "Diamond Anvil Cell, High Pressure Research", vol. 29 (2009).

[15] D.V. Semenok & al, arXiv:1902.10206 (2019).

[16] C. J. Kim, "Levitation of Magnets above Superconductors", Springer, Singapore (2019).

[17] N. Rjabinin & L.W. Schubnikow, *Physikalische Zeitschrift der Sowjetunion*, **7** (1) (1935) 22–25

[18] L. D. Landau, *Zhurnal Eksperimental'noi i Teoreticheskoi Fiziki*, **7** (1937) 19.

[19] P. Tiwar & al, *Journal of Electronic Materials*, **25**(1) (1996)131-135.

[20] W. L. McMillan, *Phys. Rev.* **167** (2) (1968) 331–344.

[21] A. Drozdov, Dissertation "Superconductivity in hydrogen-rich materials at high pressures", Johannes Gutenberg-Mainz University, (2016).

[22] J. W. Bray, "Superconductors in Applications; Some Practical Aspects," IEEE Trans. Appl. Supercond., vol. 19, pp. 2533–2539, Jun. 2009.

Chapter III :
ab initio methods

II.1. Introduction

Density functional theory (DFT) is a quantum mechanical modelling method used in Physics and Chemistry to investigate the electronic structure of many-body systems, in particular atoms, molecules, and the condensed phases. An analytical solution of the many-electron Schrödinger equation is not available, and a numerical solution, while perfectly possible in theory, is effectively impossible in practice for more than a handful of electrons due to the finite speed and memory of computers. In this section we will introduce density functional theory (DFT) as a mean of circumventing solution of the many-electron Schrödinger equation, since the properties of a many-electron system can be determined by using just functional of the electronic density.

II.2. Schrödinger equation

The ultimate goal of most approaches in solid state Physics and quantum Chemistry is the solution of the time-independent, non-relativistic Schrödinger equation

$$\hat{H}\psi_i = E_i\psi_i \tag{II.1}$$

$\hat{H}$ Is the Hamiltonian for a system consisting of M nuclei and N electrons.

$$\hat{H} = T_N + T_e + U_{ee} + U_{Ne} + U_{NN} \tag{II.2}$$

Where T_N is the nuclei kinetic energy,T_e is the electron kinetic energy, U_{ee} is the interaction energy between electrons, U_{Ne} is the interaction energy between cores and electrons, U_{NN} is the interaction energy between cores, E is the eigenvalue of the Hamiltonian, it represents the total energy of the system, Ψ is the wave function of the system, which depends on the coordinates of the cores and electrons.$\psi: \psi\left[\{\overrightarrow{R_i}\}, \{\vec{r_i}\}\right]$. Where: $\{\overrightarrow{R_i}\} = R_1, R_2, \dots, R_N$ represents the group of the cores coordinates and $\{\vec{r_i}\} = r_1, r_2, \dots, r_{Ne}$ represents the group of the electrons coordinates.

Well in atomic units, the Hamiltonian of system writing as fellow:

$$H = \left[-\frac{1}{2}\sum_{i=1}^{N}\nabla_i^2 - \frac{1}{2}\sum_{A=1}^{M}\frac{1}{M_A}\nabla_A^2 - \sum_{i=1}^{N}\sum_{A=1}^{M}\frac{Z_A}{r_{iA}} + \sum_{i=1}^{N}\sum_{j>i}^{N}\frac{1}{r_{ij}} + \sum_{A=1}^{M}\sum_{B>A}^{M}\frac{Z_A Z_B}{R_{AB}}\right] \tag{II.3}$$

Here, A and B run over the M nuclei while i and j denote the N electrons in the system. The first two terms describe the kinetic energy of the electrons and nuclei. The other three terms represent the

attractive electrostatic interaction between the nuclei and the electrons and repulsive potential due to the electron-electron and nucleus-nucleus interactions [1].

II.3. The Born-Oppenheimer approximation:

The first approximation used to solve the equation (II.1) is the adiabatic approximation made in 1926 by Born and Oppenheimer. It is based on the very large difference between the masses of nuclei and electrons (it is less than 10^{-5} for atoms heavier than calcium). Thus the electronic relaxation is instantaneous in relation to the movement of the nuclei. Then we can write the wave function of the system as a product of to wave functions, one for nuclei and the other for electrons which is the electronic wave function. Thus, the potential energy U_{NN} becomes a constant.

$$\psi\left[\{\vec{R_i}\},\{\vec{r_i}\}\right] = \psi_e\left[\{\vec{r_i}\},\{\vec{R_i}\}\right] \times \emptyset_N\left[\{\vec{R_i}\}\right] \quad \text{(II.4)}$$

We are interested in electric wave function which must satisfy the equation:

$$H_e\psi_e = E_e\psi_e \quad \text{(II.5)}$$

Where the electronic Hamiltonian can be written as follow:

$$H_e = -\frac{1}{2}\sum_{i=1}^{N}\nabla_i^2 - \sum_{i=1}^{N}\sum_{A=1}^{M}\frac{Z_A}{\overrightarrow{r_{iA}}} + \sum_{i=1}^{N}\sum_{j>i}^{N}\frac{1}{\overrightarrow{r_{ij}}} = T_e + U_{Ne} + U_{NN} \quad \text{(II.6)}$$

The solution of the Schrödinger equation with H_e is the electronic wave function Ψe and the electronic energy Ee.The total energy E_{tot} is then the sum of E_e and the constant nuclear repulsion term E_{nuc} [2].

$$E_{tot} = E_e + E_{nuc} \quad \text{(II.6)}$$

Where:
$$E_{nuc} = \sum_{A=1}^{M}\sum_{B>A}^{M}\frac{Z_A Z_B}{\overrightarrow{R_{AB}}} \quad \text{(II.7)}$$

II.4. Hartree and Hartree –Fock approximation

II.4.1.Hartree approximation:

The second approximation completed the one of Born-Oppenheimer. It was proposed by Hartree, based on the hypothesis of the free electron, where we ignore the interactions between

electrons and spin states [3]. So the electronic wave function would be written as product of mono electronic waves:

$$\psi\left[\{\vec{r_i}\},\{\vec{R_i}\}\right] = \psi_1(\vec{r_1}),\psi_2(\vec{r_2}),\dots\dots,\psi_N(\vec{r_N}) \quad \text{(II.8)}$$

The equations of solved system written as the form:

$$H_H\psi_i(\vec{r_i}) = \varepsilon_i\psi_i(\vec{r_i}) \quad \text{(II.9)}$$

$$\left(-\frac{1}{2}\nabla_i^2 + U_{ext}(\vec{R},\vec{r}) + U_H(\vec{r})\right)\psi_i(\vec{r_i}) = \varepsilon_i\psi_i(\vec{r_i}) \quad \text{(II.10)}$$

The consequences of this approximation are:

- The total Colombian repulsion is overestimated.
- There is no self-interaction.
- The Pauli principal is not respected.
- Exchange effects and correlation are ignored.

II.4.2.Hartree-Fock approximation:

To fix these consequences, Hartree and Fock proposed to express the multi-electronic wave function as a Slater determinant:

$$\psi_e = \psi_{SD} = \frac{1}{\sqrt{N!}}\begin{vmatrix} \psi_1(r_1) & \psi_2(r_1)\dots\dots & \psi_N(r_1) \\ \psi_1(r_2) & \psi_2(r_2)\cdots\cdots & \psi_N(r_2) \\ \vdots & \vdots & \vdots \\ \psi_1(r_N) & \psi_2(r_N) & \psi_N(r_N) \end{vmatrix} \quad \text{(II.11)}$$

Every wave function ψ_i is called “spin orbital” because it’s composed of two parts, the first is a special orbital function and the second is the spin function (up or down) [4].

This maneuver respects the nature of electrons (Fermions), so the Pauli principal is also respected. The Slater determinant can be obtained using the variationnal principal [4]. The application of Hamiltonian on the wave function gives the expression of Hartree-Fock energy:

$$\boldsymbol{E_{HF} = \langle\psi_{SD}|\hat{H}|\psi_{SD}\rangle = \sum_{i=1}^{N}\langle\psi_i|\hat{h}|\psi_i\rangle + \sum_{i=1}^{N}\sum_{j>i}^{N}\left[\int\int|\psi_i(r_i)|^2\frac{1}{|r_i-r_j|}|\psi_j(r_j)|^2 dr_i dr_j -\right.}$$

$$\left.\boldsymbol{\int\int\psi_i(r_i)\psi_j^*(r_j)\frac{1}{|r_i-r_j|}\psi_j(r_i)\psi_i^*(r_j)dr_i dr_j}\right] \quad \text{(II.12)}$$

Where: $$\hat{h} = -\frac{1}{2}\Delta - \sum_{i=1}^{N}\frac{Z_j}{|R_j - r|} \quad \text{(II.13)}$$

The equation (II.12) represents the kinetic energy, and the attraction energy between cores and electrons. The other two terms are respectively: the Coulomb integral which is noted by J_{ij} (called also the Hartree potential), and the exchange integral which is noted by K_{ij}. The difference of these two terms gives us the Hartree-Fock potential energy:

$$U_{HF} = \frac{1}{2}\sum_{j>i}^{N}\left[\hat{J}_J(\vec{r_i}) - \hat{K}_J(\vec{r_i})\right] \quad \text{(II.14)}$$

The consequences of Hartree-Fock approach can be sited as follow:

- The Pauli principal is respected.
- There is no self-interaction.
- It introduces the exchange effect.
- It does not take into account the correlation effect.

II.5. Density functional theory (DFT)

The density functional theory was proposed by Hohenberg and Kohn in 1964, it is a method to calculate the electronic structure of the material using the electronic density $n(\vec{r})$ instead of the N system wave function $\psi(\vec{r_1}, \vec{r_2}, \ldots, \vec{r_N})$. The idea is based on the Thomas-Fermi model (1927).

Hohenberg and Kohn firstly, and Kohn and Sham secondly allow to establish the theoretical formalism on which the current method is based. It is theory exact in its principle that allows to calculate all properties of the fundamental state. While the multi-electronic wave function depends on 3N variables, the density is only a function of three variables, which greatly reduces the time of calculations and allows to study systems of large sizes out of reach of other methods based on the wave function.

II.5.1. The Thomas-Fermi model

The conventional approaches use the wave function Ψ as the central quantity, since Ψ contains the full information of a system. However, Ψ is Avery complicated quantity that cannot be probed experimentally and that depends on 4N variables, N being the number of electrons. The Thomas-Fermi model is the first density functional theory (1927). Based on theuniform electron gas [5].

They proposed the following functional for the kinetic energy:

$$T_{TF}[n(\vec{r})] = \frac{3}{10}(3\pi^2)^{2/3}\int n^{5/3}(\vec{r})d\vec{r} \qquad \text{(II.16)}$$

The energy of an atom is finally obtained using the classical expression forthe nuclear-nuclear potential and the electron-electron potential:

$$E_{TF}[n(\vec{r})] = \frac{3}{10}(3\pi^2)^{2/3}\int n^{5/3}(\vec{r})d\vec{r} - Z\int\frac{n(\vec{r})d\vec{r}}{r} + \frac{1}{2}\int\int\frac{n(\vec{r_1})n(\vec{r_2})}{r_{1,2}}d\vec{r}_1 d\vec{r_2} \qquad \text{(II.17)}$$

The energy is given completely in terms of the electron density! In order to determine the correct density to be included in Eq. (II.17), they employed a variational principle. They assumed that the ground state of the system isconnected to the $n(\vec{r})$ for which the energy is minimized under the constraintof R $n(\vec{r}) = N$.

Despite the fact that TF theory was a rough solution to the many-electron Schrödinger equation, it was unclear whether there was a strict connection between them and whether knowledge of the ground-state density $n_0(\vec{r})$ alone uniquely determined the system [5]. This mestery was solved by Hohenberg and Kohn.

II.5.2.The Hohenberg-Kohn theorem

The Hohenberg-Kohn theorems relate to any system consisting of electrons moving under the influence of an external potential $U_{ext}(\vec{r})$[6].

Stated simply they are as follows:

Theorem 01:

The first Hohenberg-Kohn theorem demonstrates that the electron density uniquely determines the Hamiltonian operator and thus all the properties of the system. This first theorem states that the external potential $U_{ext}(\vec{r})$ is (to within a constant) a unique functional of $n(\vec{r})$, in turn $U_{ext}(\vec{r})$ fixes H we see that the full many particle ground-state is a unique functional of *n(r)*.And so that there cannot be two different $U_{ext}(\vec{r})$ that give the same $n(\vec{r})$for their ground state. Thus, $n(\vec{r})$ determines N and $U_{ext}(\vec{r})$ and hence all the properties of the ground state, for example the kinetic energy *T [n(r)]*, the potential energy *U* $[n(\vec{r})]$, and the total energy *E* $[n(\vec{r})]$.

Now, we can write the total energy as:

$$E[n(\vec{r})] = \langle\psi|H|\psi\rangle = F_{HK}[n(\vec{r})] + \int U_{ext}(\vec{r}).n(\vec{r})dr \quad \text{(II.18)}$$

With:
$$F_{HK}[n(\vec{r})] = T_e[n(\vec{r})] + U_{ee}[n(\vec{r})] \quad \text{(II.19)}$$

Where: F_{HK}: the Hohenberg-Kohn functional that represents the Coulombian and kinetic contributions in the energy (F_{HK} is dependent of the external potential applied on the system).

T_e: the kinetic energy and U_{ee}: electron-electron interaction.

Theorem 02:

According to the variationnal principle, the electronic density of the system in the ground-state minimizes the total energy of this system:

$$E_0[n(\vec{r})] = minE[n(\vec{r})] \quad \text{(II.20)}$$

It must satisfy the following conditions:

- ✓ $n(\vec{r}) \geq 0.$
- ✓ $\int_{\Omega} n(\vec{r}).d^3\vec{r} = N_e$

Where: E_0 is the total energy in the ground-state, Ω is the volume system and N_e is the number of electrons [6].

II.5.3. The Kohn-Sham approach

In 1965, Kohn and Sham proposed a new method allows to use the DFT. First, they supposed that the electronic density of the real system is equal to the one of fictitious system composed of particles without interactions [7].

To calculate $n_0(\vec{r})$ and the system energy, they replaced the original problem:

$$\text{E: } \begin{cases} H\psi_i = E\psi_i \\ n_0(\vec{r}) = \int d^3r_1 \ldots\ldots, d^3r_N |\psi_i(\overrightarrow{r_1}, \ldots., \overrightarrow{r_N}|^2 \end{cases} \quad \text{(II.24)}$$

By:
$$\text{E': } \begin{cases} H_{KS}\psi_j(\vec{r}) = \varepsilon_j\psi_j(\vec{r}) \Leftrightarrow \left(\frac{-\hbar^2\nabla^2}{2m} + U_{eff}\right)\psi_j(\vec{r}) = \varepsilon_j\psi_j \\ n_0(\vec{r}) = \sum_{j=1}^{N}\left[\psi_j(\vec{r})\right]^2 \end{cases} \quad \text{(II.25)}$$

The problem E' is simpler than the problem E because:

- We solved a Schrödinger equation with a single particle (mono-electronic) using the potential U_{eff} which makes it possible to obtain the second equation from Kohn-Sham to Ne states.
- The expression of electronic density is given according to N_e wave functions ψ_j **,** it's the third Kohn-Sham equation.

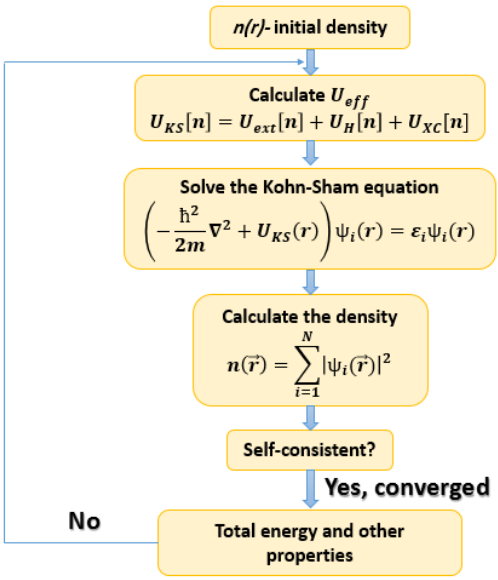

Fig II.1: Flowchart of DFT self-consistent cycle calculation.

II.10. Exchange-correlation functional

II.10.1. The local density approximation (LDA):

The simplest approximation is to assume that the density can be treated locally as a uniform electron gas, the exchange correlation energy at each point in the system is the same as that of a uniform electron gas of the same density. This approximation was originally introduced by Kohn and Sham and holds for a slowly varying density [8].

Using this approximation the exchange-correlation energy for a density $n(\vec{r})$ is given by:

$$E_{XC}^{LDA} = \int n(\vec{r})\varepsilon_{xc}[n(\vec{r})]d\vec{r} \qquad \text{(II.26)}$$

Where: $\varepsilon_{xc}[n(\vec{r})]$ is the exchange-correlation per particle for a uniform electron gas of density $[n(\vec{r})]$.

The exchange-correlation potential is then given by:

$$v_{xc}^{LDA}[n(\vec{r})] = \frac{\delta E_{xc}^{LDA}}{\delta n(\vec{r})} = \varepsilon_{xc}[n(\vec{r})] + n(\vec{r})\frac{\partial \varepsilon_{xc}[n(\vec{r})]}{\partial n(\vec{r})} \quad \text{(II.27)}$$

For practical use of the LDA in calculations it is necessary to determine the exchange-correlation energy for a uniform electron gas of a given density [8].

II.6.2. Generalized gradient approximation:

A method to approximate both the exchange and correlation energy in density functional methods and represent a further development of local density approximation (→ LDA).

The GGA is a higher level approximation of the exchange correlation energy functional where the exchange correlation energy, E_{xc}, is an integral over all space with the exchange correlation energy density, ε_{xc}, depending on both the local electronic density and its gradient as shown in the equation below:

$$E_{xc}^{GGA}[n(\vec{r})] = \int n(\vec{r})\varepsilon_{xc}[n(\vec{r}), |\nabla^m n(\vec{r})|]d^3\vec{r} \quad \text{(II.28)}$$

The term, GGA, denotes a variety of ways proposed for functions, $\varepsilon_{xc}[n(\vec{r}),|\nabla^m n(\vec{r}))|]$, that modify the behavior at large gradients in such a way as to preserve desired properties.Several work has been done in the spirit of LDA and GGA to get a better approximation of *Exc* [9].

II.11. DFT in crystalline systems

II.11.1. Born-von Karman periodic boundary conditions:

Born–von Karman boundary conditions are periodic boundary conditions which impose the restriction that a wave function must be periodic on a certain Bravais lattice. Named after Max Born and Theodore von Karman. This condition is often applied in solid state physics to model an ideal crystal. Born and von Karman published a series of articles in 1912 and 1913 that presented one of the first theories of specific heat of solids based on the crystalline hypothesis and included these boundary conditions [10].

The condition can be stated as:

$$\psi(\vec{r} + N_i\overrightarrow{a_i}) = \psi(\vec{r}) \quad \text{(II.29)}$$

Where *i* runs over the dimensions of the Bravais lattice, the $\overrightarrow{\boldsymbol{a_i}}$ are the primitive vectors of the lattice, and the N_i are integers (assuming the lattice has *N* cells where $N=N_1N_2N_3$). This definition can be used to show that:

$$\psi\left(\vec{r} + \vec{T}\right) = \psi(\vec{r}) \quad \text{(II.30)}$$

For any lattice translation vector $\vec{T}$ such that:

$$\vec{T} = \sum_i N_i\overrightarrow{a_i} \quad \text{(II.31)}$$

The Born–von Karman boundary condition is important in solid state physics for analyzing many features of crystals, such as diffraction and the band gap. Modeling the potential of a crystal as a periodic function with the Born von Karman boundary condition and plugging in Schrödinger's equation results in a proof of Bloch's theorem, which is particularly important in understanding the band structure of crystals [10].

II.11.2. Bloch's theorem:

Thus far, the quantum mechanical approaches to solving the many-body problem have been discussed. However, the correlated nature of the electrons within a solid is not the only obstacle to solving the Schrödinger equation for a condensed matter system: for solids, one must also bear in mind the effectively infinite number of electrons within the solid. One may appeal to Bloch's theorem in order to make headway in obviating this latter problem. Instead of being required to consider an infinite number of electrons, it is only necessary to consider the number of electrons within the unit cell (or half of this number if the electrons are spin degenerate) [11].

Bloch's theorem states that the wave function of an electron within a perfectly periodic potential may be written as:

$$\psi_{j,k}(\vec{r}) = u_j(\vec{r})e^{i.\vec{r}.\vec{k}} \quad \text{(II.32)}$$

Where: $u_j(\vec{r})$ is a function that possesses the periodicity of the potential, *i.e.:* $u_j(\vec{r}+\vec{l}) = u_j(\vec{r})$ where *l* is the length of the unit cell.*j*is the band index, and *k* is a wave vector confined to the first Brillouin Zone.

Since $u_j(\vec{r})$ is a periodic function, we may expand it in terms of a Fourier series:

$$u_j(\vec{r}) = \sum_G c_j.Ge^{i\vec{G}.\vec{r}} \quad \text{(II.33)}$$

Where *G* are reciprocal lattice vectors defined through *G.R=2πm, m* is an integer, *R* is real space lattice vector and $c_j.G$ are plane wave expansion coefficients. The electron wave functions may therefore be written as a linear combination of plane waves:

$$\psi_{j,k}(\vec{r}) = \sum_G c_{j,k}.Ge^{i(\vec{k}+\vec{G})\vec{r}} \quad \text{(II.34)}$$

Given that each electron occupies a state of definite *k*, the infinite number of electrons within the solid gives rise to an infinite number of k-points. At each k-point, only a finite number of the available energy levels will be occupied. Thus one only needs to consider a finite number of electrons at an infinite number of k-points. This may seem to be replacing one infinity (number of electrons) with another one (number of k-points) to little discernible advantage. However, one does not need to consider all of these k-points, rather, since the electron wave functions will be almost identical for values of *k* that are sufficiently close, one can represent the wave functions over a region of reciprocal space by considering the wave function at a single k-point. It is therefore sufficient to consider the electronic states at a finite number of k-points in order to determine the ground-state density of the solid. The net effect of Bloch's Theorem therefore has been to change the problem of an infinite number of electrons to one of considering only the number of electrons in the unit cell (or half that number, depending on whether the states are spin-degenerate or not) at a finite number of k-points chosen so as to appropriately sample the Brillouin Zone [11].

II.11.3. Brillouin zone:

The first Brillouin zone is a uniquely defined primitive cell in reciprocal space. In the same way the Bravais lattice is divided up into Wigner–Seitz cells in the real lattice, the reciprocal lattice is

broken up into Brillouin zones. The boundaries of this cell are given by planes related to points on the reciprocal lattice. The importance of the Brillouin zone stems from the Bloch wave description of waves in a periodic medium, in which it is found that the solutions can be completely characterized by their behavior in a single Brillouin zone.

The first Brillouin zone is the locus of points in reciprocal space that are closer to the origin of the reciprocal lattice than they are to any other reciprocal lattice points (see the derivation of the Wigner-Seitz cell). Another definition is as the set of points in *k*-space that can be reached from the origin without crossing any Bragg plane.

There are also second, third, *etc.*, Brillouin zones, corresponding to a sequence of disjoint regions (all with the same volume) at increasing distances from the origin, but these are used less frequently. As a result, the first Brillouin zone is often called simply the Brillouin zone. In general, the *n*-th Brillouin zone consists of the set of points that can be reached from the origin by crossing exactly $n - 1$ distinct Bragg planes. A related concept is that of the irreducible Brillouin zone, which is the first Brillouin zone reduced by all of the symmetries in the point group of the lattice (point group of the crystal) [12].

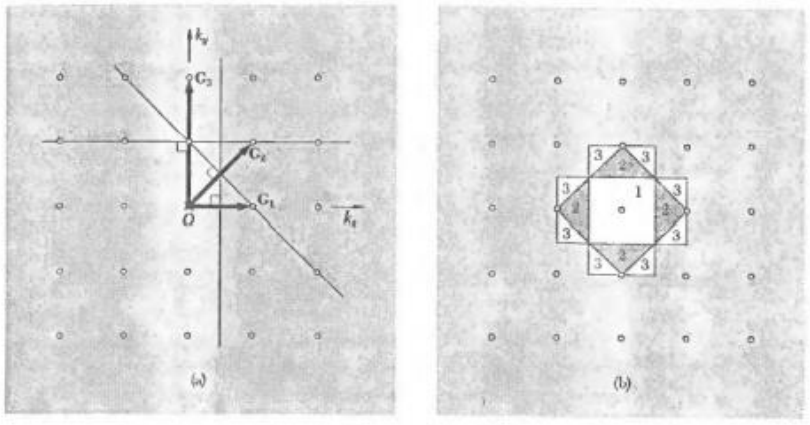

Figure **II.2**: illustration of Brillouin zones [11].

Since the end of the sixties it is known that the constants of force crystal harmonics can be determined by their electronic response. Hence, the essential approximation, which allows the decoupling of the atomic vibrations of electronic degrees of freedom in the solid, is adiabatic approximation of Born and Oppenheimer. Thus, according tothis approximation, the lattice

distortions in a crystal associated with a phonon can be seen as a static disturbance acting on the electrons [12].

II.12. The pseudo-potential and plane waves approach

II.12.1. Plane waves bases:

Plane wave bases, associated with periodic boundary conditions, areoften suitable for the study of solids in so far as they satisfy by construction the Bloch's theorem. Plane wave decomposition of wave functions $\psi_{j,k}(r)$ consists of expressing these wave functions using Fourier series:

$$\psi_{j,k}(\vec{r}) = \Omega^{-1/2} \sum_G C_j^k(\bar{G}) e^{i(\bar{K}+\bar{G}).\vec{r}} \quad \text{(II.35)}$$

Theoretically, it would be necessary to use an infinite base of plane waves, but in practice, the serial development is truncated to a certain term which is defined by the cutoff energy E_{cut}. More precisely, we limit ourselves to plane waves with a kinetic energy less than $E_{cut.}$

$$\frac{\hbar}{2m}|K+G| < E_{cut} \quad \text{(II.36)}$$

An increase in E_{cut} allows the base to be extended and improve accuracy of the calculation, but obviously leads to an increase in calculation time. The energy of minimal cut-off allowing correct treatment of the problem depends on the pseudo-potential used and the system studied, so that it is necessary to perform convergence studies before interpreting results [13].

II.12.2. Pseudopotentials:

In solid molecules and compounds, valence electrons are the only act in the chemical bonds, the electrons of the core, which are on the deepest and close to the core are very sensitive to the environment, and are difficult to represent on a plane wave basis because they usually have strong oscillations around the core. We can now group the electrons of the heart with the nuclei, to form rigid ions, whose electronic states will remain unchanged whatever the environment in which the atom will be placed. It is the approximation of the frozen core. We can go further by replacing the interaction of valence electrons with the group {nucleus and electrons of core} by an effective potential, much less attractive than the potential created by the nucleus with all electrons, this actual potential is called a pseudopotential [14].

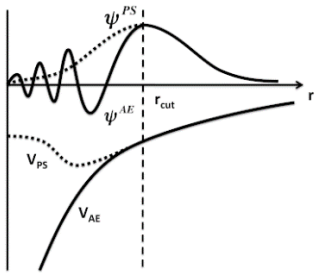

Figure **II.3**: Schematic representation of the pseudopotential method [13].

Fig.II.3 Shows variations in wave function and potential in both atomic regions as a function of distance (r) from the nuclei, and the correlation between both methods AE (all electrons) and PS (pseudopotential) from certain distance of the core, this distance is known as r_{cut}. Inside r_{cut} region, the wave function is replaced by pseudo wave function which is conceived to simplify calculations. Outside of the previous region, the full wave function and the pseudo wave function must be coincided in calculations of a given atomic state. The PS method reduces the calculation volume and abridge the execution period by minimizing electrons number in calculation and plane waves number required to describe the wave functions in solid [13].

II.9. Density Functional Perturbation Theory

All the physical properties of a system (a crystal in our case) represent the system response to external disturbance (atomic displacement, electric field, deformation...), then these properties are only the change that undergoes the total energy of the disrupted system. They are directly related to total energy derivatives compared to one (or more) disturbance(s).

Derivatives of total energy (electronic part + nuclei-nuclei interaction):

1st order derivatives: forces, stresses, dipole moment...

2nd order derivatives: dynamical matrix, elastic constants, dielectric susceptibility atomic polar tensors or Born effective charge tensors piezoelectricity, internal strains.

3rd order derivatives: non-linear dielectric susceptibility, Raman susceptibilities electro-optic effect, phonon - phonon interaction, Grüneisen parameters.

Further properties obtained by integration over phononic degrees of freedom: entropy, thermal expansion, phonon-limited thermal conductivity... [14].

If we considered that U_{ext} is depends on a set of adiabatic perturbation parameters

$\Lambda = \{\lambda_a, a = 1, \dots, p\}$. Each U_{ext}^{Λ} determines an electronic ground-state with density $n^{\Lambda}(\vec{r})$ and total energy $E^{\Lambda} = F[n^{\Lambda}] + \int d^3r\, n^{\Lambda}(\vec{r}) U_{ext}^{\Lambda}(\vec{r})$ which depends on theperturbation via the external potential and implicitly via the density.

Its derivative then contains two contribution:

$$\frac{\partial E^{\Lambda}}{\partial \lambda_a} = \int d^3r\, n^{\Lambda}(\vec{r}) \frac{\partial U_{ext}^{\Lambda}(\vec{r})}{\partial \lambda_a} + \int d^3r \frac{\delta E^{\Lambda}}{\delta n(\vec{r})} \frac{\partial\, n^{\Lambda}(\vec{r})}{\partial \lambda_a} \qquad \text{(II.37)}$$

Due to the variational principle, the second term vanishes for each finite Λ. Thus the first derivative depends on the ground-state density only. This represents the DFT equivalent of the well-known Hellman-Feynman-Theorem [15].

The second-order derivatives are then given by:

$$\frac{\partial^2 E^{\Lambda}}{\partial \lambda_a \partial \lambda_b} = \int d^3r \frac{\partial n^{\Lambda}(\vec{r})}{\partial \lambda_b} \frac{\partial U_{ext}^{\Lambda}(\vec{r})}{\partial \lambda_a} + \int d^3r\, n^{\Lambda}(\vec{r}) \frac{\partial^2 U_{ext}^{\Lambda}(\vec{r})}{\partial \lambda_a \partial \lambda_b} \qquad \text{(II.38)}$$

For practical purposes it is important that the second derivatives require only the knowledge ofthe first-order variations of the electron density. Therefore, it is sufficient to consider only the linear response of the electron system.

II.10. First principals phonon calculations

Due to the progress of high performance computers and development of efficient density functional theory (DFT) codes, application of first principals' calculations in condensed matter physics has greatly expanded when phonon calculations became routine in last decade. Equilibrium crystal structures can be obtained by minimizing residual forces and optimizing stress tensors. When an atom in a crystal is displaced from its equilibrium position, the forces on all atoms in the crystal raise. Analysis of the forces associated with a systematic set of displacements provides a series of phonon frequencies. First principles phonon calculations with finite displacement method (FDM) [16, 17] can be made in this way. An alternative approach for phonon calculations is the density

functional perturbation theory (DFPT) [18, 19]. The information of phonon is very useful for accounting variety of propreties and behaviors of crystalline materials (thermal propreties, phase transition and superconductivity…).

a. Harmonic approximation:

As known, in the crystal atoms move around their equilibrium position, crystal potential energy $\boldsymbol{\Phi}$ is presumed to be analytic function of the displacements of atoms. $\boldsymbol{\Phi}$ is expended as:

$$\Phi = \Phi_0 + \sum_{lk}\sum_{\alpha}\Phi_{\alpha}(lk)\overrightarrow{u_{\alpha}}(lk) + \frac{1}{2}\sum_{ll'kk'}\sum_{\alpha\beta}\Phi_{\alpha\beta}(lk,l'k')\overrightarrow{u_{\alpha}}(lk)\overrightarrow{u_{\beta}}(l'k') + \frac{1}{3!}\sum_{ll'l''kk'k''}\sum_{\alpha\beta\gamma}\Phi_{\alpha\beta\gamma}(lk,l'k',l''k'')\overrightarrow{u_{\alpha}}(lk)\overrightarrow{u_{\beta}}(l'k')\overrightarrow{u_{\gamma}}(l''k'') \ldots \quad \text{(II.39)}$$

Where: $\vec{u}(lk)$is the displacement vector, *l* and *k* are the labels of unit cells and atoms in each unit cell, $\boldsymbol{\alpha}$, $\boldsymbol{\beta}$, $\boldsymbol{\gamma}$ are Cartesian indices, the coefficients of series expansion Φ_0, Φ_{α}, $\Phi_{\alpha\beta}$, $\Phi_{\alpha\beta\gamma}$ are the zeroth, first, second and third order force constants with a small displacement at a constant volume.

The problem of atomic vibrations is solved with 2nd order terms as the harmonic approximation, and the high order terms are treated by the perturbation theory.The dynamical property of atoms in the harmonic approximation is obtained by solving eigenvalue problem of dynamical matrix [20, 21]:

$$\sum_{\beta k'} D_{kk'}^{\alpha\beta}(q)e_{qj}^{\beta k'} = \omega_{qj}^2 e_{qj}^{\alpha k} \quad \text{(II.40)}$$

$$\text{With: } D_{kk'}^{\alpha\beta}(q) = \sum_{l'}\frac{\Phi_{\alpha\beta}(0k,l'k')}{\sqrt{m_k m_{k'}}}e^{iq.[r(l'k')-r(0k)]} \quad \text{(II.40)}$$

Where: m_k is the mass of the atom *k*, q is the wave vector, and *j* is the band index. ω_{qj} And ω_{qj} give the phonon frequency and polarization vector of the phonon mode labeled by a set $\{q, j\}$ respectively. Since *D(q)* is an Hermitian matrix, its eigenvalues ω_{qj}^2 are real. Usually, *D(q)* is arranged to be a $3n_a \times 3n_a$ matrix [21], where 3 comes from the freedom of the Cartesian indices for crystal and n_a is the number of atoms in a unit cell. Then e_{qj} becomes a complex column vector with $3n_a$ elements. And usually e_{qj} is normalized to be 1, e_{qj} contains information of collective motion of atoms.

This may be understood as a set of atomic displacement vectors:

$$[u(l1),\dots,u(lk)] = \left[\frac{A}{\sqrt{m_1}} e_{qj}^{1} e^{iq.r(l1)},\dots,\frac{A}{\sqrt{m_{n_a}}} e_{qj}^{n_a} e^{iq.r(lk)}\right] \quad \text{(II.41)}$$

Where A is the complex constant undetermined by equ (II.40).

As a typical example, the phonon band structure and phonon density of states (DOS) of Al are shown in Fig. II.4.the phonon DOS is defined as:

$$g(\omega) = \frac{1}{N}\sum_{qj} \delta(\omega - \omega_{qj}) \quad \text{(II.41)}$$

Where N is the number of unit cells in crystal. Divided by N, $g(\omega)$ is normalized so that the integral over frequency becomes $3n_a$.

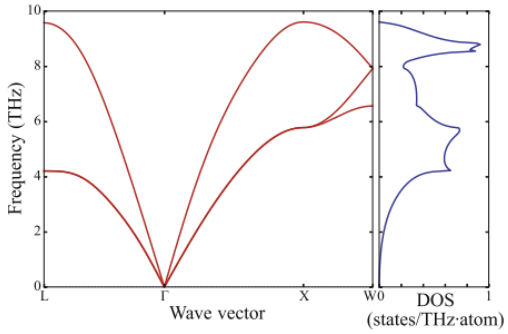

Figure 0: Phonon band structure and DOS

Atom specific phonon DOS projected along a unitdirection vector $\hat{n}$ is defined as:

$$g_k(\omega,\hat{n}) = \frac{1}{N}\sum_{qj} \delta(\omega - \omega_{qj})\left|\hat{n}.e_{qj}^{k}\right|^2 \quad \text{(II.42)}$$

Once phonon frequencies over Brillouin zone are known, fromthe canonical distribution in statistical mechanics for phonons under the harmonic approximation, the energy E of phonon systemis given as:

$$E = \sum_{qj} \hbar\omega_{qj}\left[\frac{1}{2} + \frac{1}{\exp(\hbar\omega_{qj}/k_B T)-1}\right] \quad \text{(II.43)}$$

Where: T is the temperature, k_B is Boltzmann constant and ħ is the reduced Planck constant.

b. Stability condition and imaginary mode:

At equilibrium $\frac{\partial \Phi}{\partial r_\alpha(lk)} = 0$ a crystal is dynamically stable if its potential energy always increases against any combinations of atomic displacements. In the harmonic approximation, this is equivalent to the condition that all phonons have real and positive frequencies [22]. However under virtual thermodynamic conditions, imaginary frequency or negative eigenvalue can appear in the solution of Eq. (II.40).This indicates dynamical instability of the system, which means that the corrective atomic displacements of Eq. (II.42) reduce the potential energy in the vicinity of the equilibrium atomic positions.

In such a case, the perturbation approach is invalid. Phonons with large atomic displacements may be treated by self-consistent phonon method [22, 23] or by a combination of molecular dynamics and lattice dynamics calculation [24–25]. A given structure having imaginary phonon modes can be led to alternative structures through continuous atomic displacements and lattice deformations.

References

[1] K. G. Dyall and K. Fægri Jr. Introduction to relativistic quantum chemistry. OxfordUniversity Press. Oxford, (2007). .

[2] M. Born and R. Oppenheimer, Ann. Physik. (1927), 84, 457.

[3] D. R. Hartree, Proc. Cambridge Philos. Soc. (1928), 24, 89.

[4] V. Fock, Z. Phys. (1930), 61, 126.

[5] E. Fermi. Z. Phys. (1928), 48, 73–79.

[6] P. Hohenberg and W. Kohn, Phys. Rev. B. (1964), 136, 864.

[7] W. Kohn and L. Sham, Phys. Rev. A. (1965), 140, 1133.

[8] R. Parr and W. Yang, Density-Functional Theory of Atoms andMolecules (PUBLISHER, Oxford University Press, New York, (1989).

[9] A. St-Amant, W. D. Cornell, P. A. Kollman, and T. A. Halgren J. Comput. Chem. 16, 1483 (1995)25

[10] N. W. Ashcroft, N. D. Mermin. “Solid State Physics”. Saunders College Publishing. (1976).

[11] Kittel, Charles *(1996). Introduction to Solid State Physics. New York: Wiley.* ISBN 0-471-14286-7.

[12] H .J. Monkhorst and J .D. Pack, Phys. Rev. B. (1976), 13 (12), 5188.

[13] B. Meyer. NIC Series, Vol. 31, ISBN 3-00-017350-1, pp. 71-83, (2006).

[14] B .LAGOUN. Thèse de Doctorat. CALCUL ab-initio DES PROPRIÉTÉS PHYSIQUES DE QUELQUES NOUVEAUX MATERIAUX POTENTIELS, (2015)

[15] R.P. Feynman, Phys. Rev. 56, 340 (1939)

[16] G. Kresse, J. Furthmüller, J. Hafner, Europhys. Lett. 32 (1995) 729.

[17] K. Parlinski, Z.Q. Li, Y. Kawazoe, Phys. Rev. Lett. 78 (1997) 4063.

[18] P. Giannozzi, S. de Gironcoli, P. Pavone, S. Baroni, Phys. Rev. B 43 (1991) 7231.

[19] X. Gonze, C. Lee, Phys. Rev. B 55 (1997) 10355.

[20] J.M. Ziman, Electrons and Phonons, Oxford University Press, (2001).

[21] M.T. Dove, Introduction to Lattice Dynamics, Cambridge University Press,(1993).

[22] D.C. Wallace, Thermodynamics of Crystals, Dover Publications, (1998).

[23] I. Errea, M. Calandra, F. Mauri, Phys. Rev. B 89 (2014) 064302.

[24] C.Z. Wang, C.T. Chan, K.M. Ho, Phys. Rev. B 42 (1990) 11276.

[25] T. Sun, D.-B. Zhang, R.M. Wentzcovitch, Phys. Rev. B 89 (2014) 094109.

Chapter III:
Results and discussion

III.4. Introduction

In this thesis, we take the famous compound YH_6 as a subject of study. We considered the impact of pressure on the thermodynamic stability and we used the obtained phonon frequencies to evaluate the transition temperature and the superconducting gap. The results of our calculations, based on the Density Functional Theory (DFT) [1, 2] and the Density Functional Perturbation Theory (DFPT) [3], of the structural, vibrational and superconducting parameters are presented in this chapter.

III.5. Synthesis and superconductivity of the yttrium hexahydride YH_6:

In the work of Liu et al [4], stability and conditions of existence of YH_6 in the sodalite-like crystal prototype$Im\bar{3}m$ with hexagonal H_6 units was predicted to be stable at pressures over 110 GPa. The Tc was found via numerical solution of Eliashberg equations [5] to be in range 251-264 K° at 120 GPa (μ^*=0.1-0.13) and the electron-phonon coupling parameter λ= 2.93 (120 GPa). The calculated lattice constant was found to be *a*=3.602 A° at Pressure P=150 GPa. In 2018, the study of YH_6 was continued by Grishakav et al. [6]. The lower transition parameters were: λ= 3.0, T_c= 165 K° (125 GPa). The major contribution of density of electronic states at Fermi level comes from s-d orbitals. In 2019, the most detailed study of physical propreties and superconductivity of $Im\bar{3}m - YH6$, made by Hail et al. [7]. Almost isotropic superconducting gap resulting from uniform distribution of the coupling over states of both Y and H sublattices was found. According to provided calculations, the Coulomb pseudo-potential μ^*= 0.11, T_c= 290 K° (300 GPa), the H-H distance is 1.19 A° at (300 GPa), λ= 1.73, average superconducting gap Δ= 50-55 meV. The paper of Troyan In 2019 [8], combined experimental and theoretical results. To measure the superconducting transition temperature authors used diamond anvils cells (DAC) applying different pressures. The measured superconducting transition temperature is Tc= 224 k° (166 GPa), lattice parameter is *a*= 3.573 A° (165 GPa) and the Debye temperature Θ_D = 908 (150 GPa). The calculated elastic constants at 150 GPa, 165 GPa and 180 GPa obey generalized Born-Huang conditions indicating the mechanical stability of the $Im\bar{3}m - YH6$ phase.

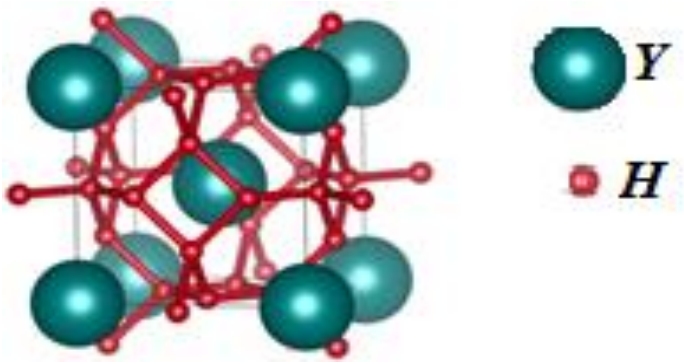

Fig III.5: Cell structure of $im\bar{3}m$-YH_6 [8].

III.3. Method of calculation:

We projected to predict the structural and vibrational properties of YH_6. Thus, we used the calculated phonon frequencies to assess the transition temperature. Calculations were performed by means ABINIT code [9] based on the Density Functional Theory (DFT). For the exchange and correlation potential we have used the generalized gradient approximation (GGA) in the Perdew-Burke-Ernzerhof (PBE) framework [10]. To approximate the interactions between valence electrons and core electrons on one side and the nucleus on another side the pseudo-potentials used for H and Ca atoms are the Troullier-Martins norm-conserving scheme. Our calculations were performed using a 6×6×6 k-point grid according to the method of Monkhorst and Pack [11]. We have used a plane wave base parameterized by a cut-off energy of 60 Ha ($E_{cut\text{-}off} \approx 1633$ *eV*). We have employed the Density Functional Perturbation Theory (DFPT) to determine the vibrational properties and the electron-phonon coupling (EPC). The states 1*s* and [Kr]: $4d^1\ 5s^2$ are treated as valence electrons for H and Y, respectively.

III.4. Structural propreties:

With the aim to characterize the structural propreties, we have to study the volume as a function of pressure. First, we must obtain the optimal volume at zero pressure, so we performed a geometric optimization of volume at zero pressure where he optimized structure corresponds to the minimal energy. In order to define this structure, we calculated variation of the total energy according to the mesh volume which is represented in Fig. III.2.

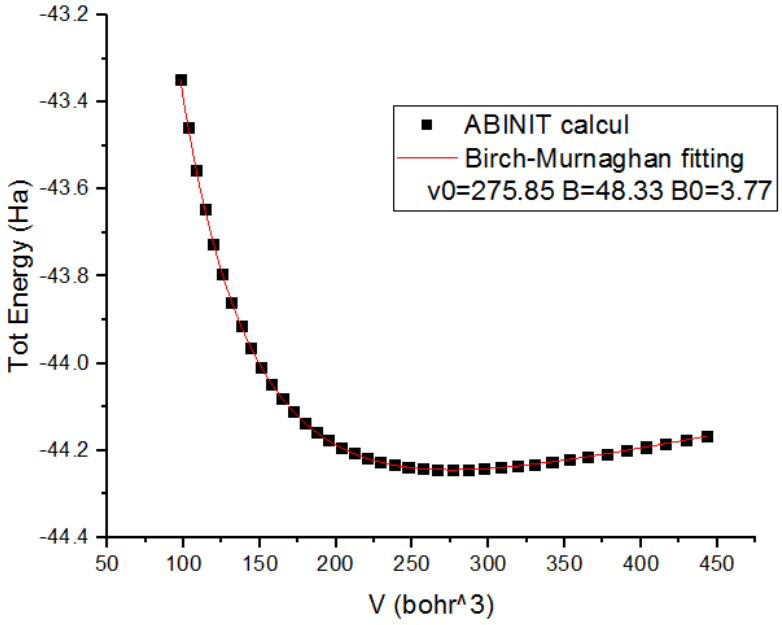

Fig III.2: variation of the total energy as a function of volume for YH6

The previous graph is based on the expression of total energy which is integrated from the one of the pressure that is written as:

$$E(V) = E_0 + \frac{9V_0B_0}{16}\left\{\left[\left(\frac{V_0}{V}\right)^{\frac{2}{3}} - 1\right]^3 B_1 + \left[\left(\frac{V_0}{V}\right)^{\frac{2}{3}} - 1\right]^2 \left[6 - 4\left(\frac{V_0}{V}\right)^{\frac{2}{3}}\right]\right\} \qquad \textbf{(III.1)}$$

Where:

E is the energy, **V** is the deformed volume, $\mathbf{V_0}$is the reference volume, $\mathbf{B_0}$ is the bulk modulus and $\mathbf{B_1}$ is the derivative of the bulk modulus with respect to the equilibrium pressure.

The Figure III.3 shows the compressibility variation depending on volume of the YH_6 compound. This result corresponds to the third order Birch-Murnaghan equation of state which is written as following [12]:

$$P(V) = \frac{3B}{2}\left[\left(\frac{V_0}{V}\right)^{\frac{7}{3}} - \left(\frac{V_0}{V}\right)^{\frac{5}{3}}\right]\left\{1 + \frac{3}{4}(4 - B_0)\left[\left(\frac{V_0}{V}\right)^{\frac{2}{3}} - 1\right]\right\} \qquad \textbf{(III.2)}$$

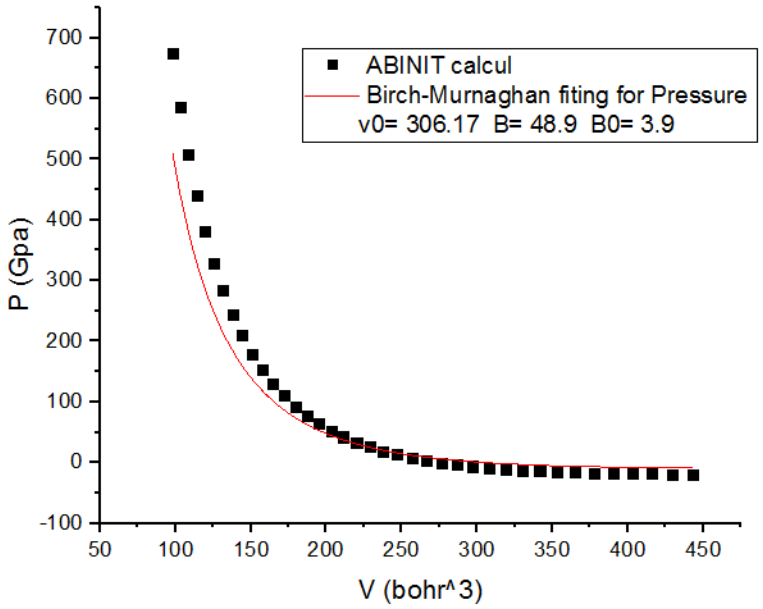

Fig. III.3: variation of the pressure as a function of volume for YH_6

As it was expected, we noted a decrease in the value of cell's parameter by increasing the stress. In the table III.1, we present the obtained lattice parameters for different pressures. It also contains a comparison with the results of previous studies. Our results appearing somewhat remote compared to the available data. This is due to the insufficient of the calculation parameters approved and this will surely negatively affect all subsequent results.

Table III.1: Lattice parameter in (A°) at different pressure values.

P (GPa)	Previous studies	This study
0	-	3.175
100	-	2.963
120	3.7 [1]	2.921
150	3.602 [2]	2.868
165	3.573 [2]	2.645
180	3.546 [2]	2.645
200	-	2.645
250	-	2.645
300	-	2.645
350	-	2.11

III.5. Vibrational properties:

a. Phonon spectrum:

In a stable periodic lattice, phonons are characterized by positive frequencies ω ***(k,v)***, where ***k*** is the wave vector and *v* denoting the polarization (longitudinal and transversal modes) and the phonon branches (acoustic and optical). Our calculations of the phonon dispersion along the main path on the Brouillon zone with DFPT allowed to obtain phonon frequencies for different values of cell parameters that correspond to some values of pressures extends from 150 GPa to 300 Gpa. According to our results, the non-existence of negative frequencies means that the structure is dynamically stable. Our result puts us on the same side with the experimental and theoretical studies previously mentioned [4, 6-8]. According to the figure III.4, there is a large band gap between the acoustic and optical modes that refers to the big difference mass of Y ions and H ions. Thus, we noticed that the gap split up the acoustic and optical modes, is gradually expands with increasing the pressure values.This indicates that the distance between the ions that make up the compound or the matrix of elastic constants plays a large role in the thermodynamic state and the superconductivity of the material.

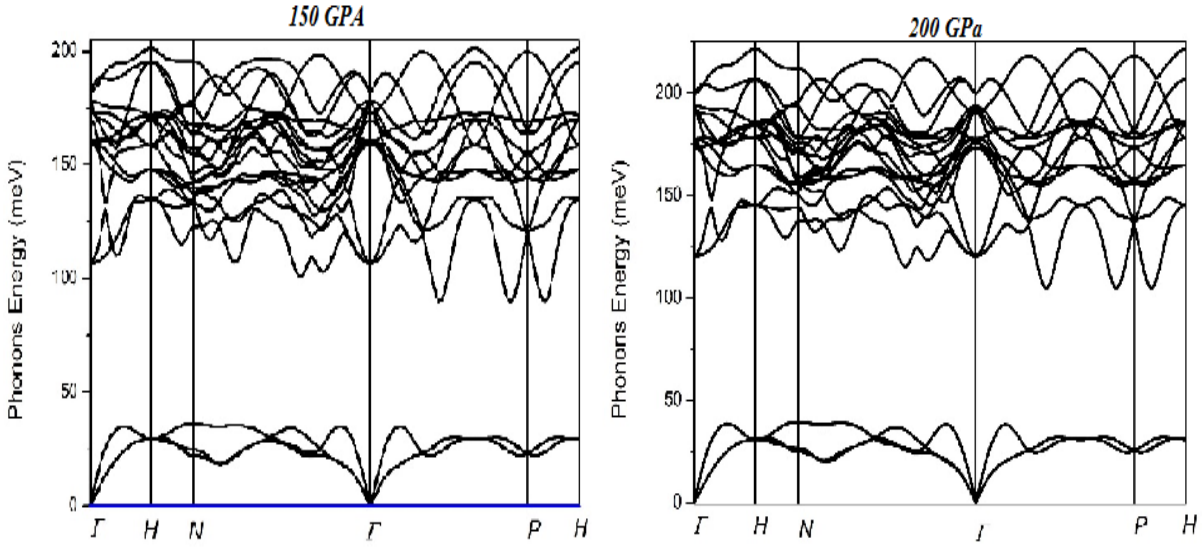

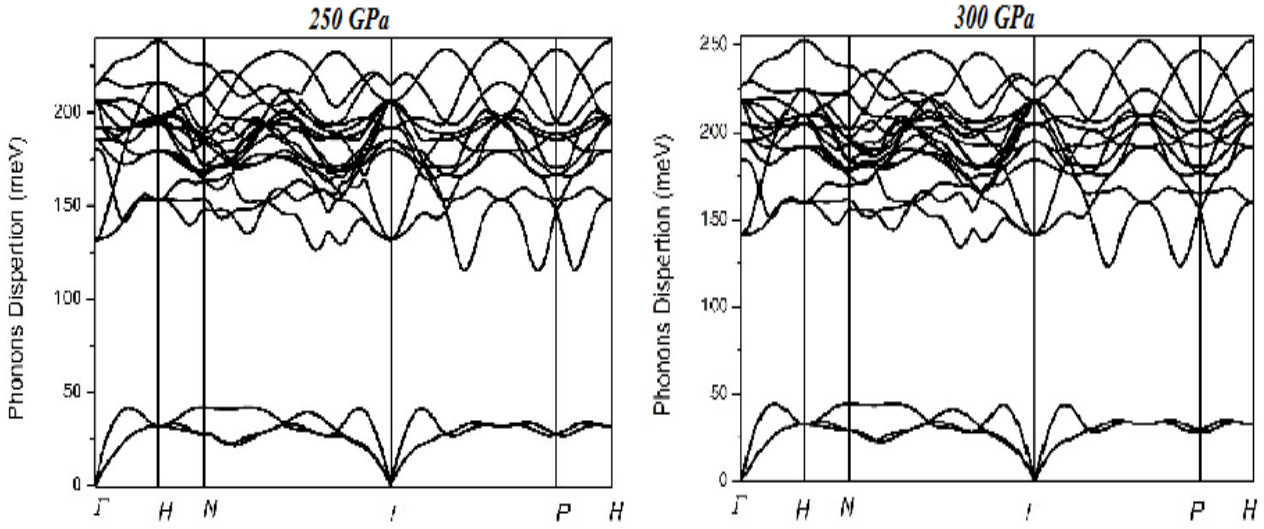

Fig III.4: Phonon spectrums of YH_6 at different pressures.

b. Phonon density of states (DOS):

To accomplish our comprehension of the phonon spectrum, we have interested to the atomic contributions to the vibrational properties. In the figure III.5, we obtained the TDOS and PDOS diagrams at different pressure values. These curves show that the vibrations of the Y atoms dominate the acoustic mode while, the optic mode is governed by H atoms vibrations. Generally, the first mode extends from zero to values not exceeding 50 meV and the second mode prolong from 95 to 250 meV. These areas increase and decrease depending on the applied pressure.

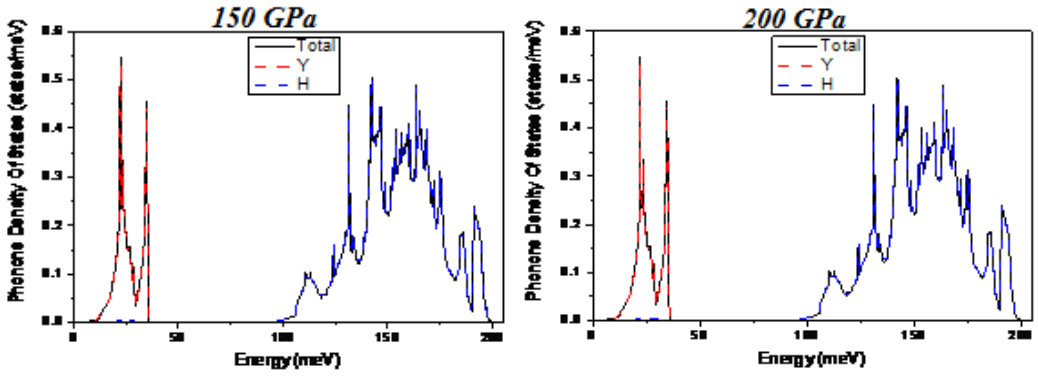

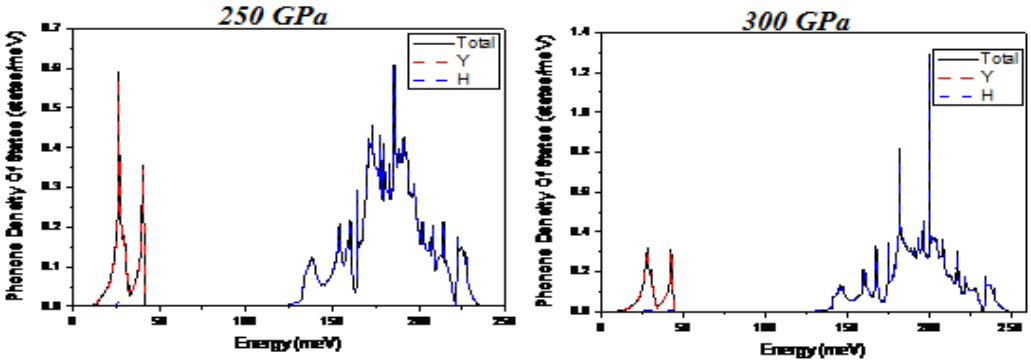

Fig III.5: total DOS and partial DOS diagrams of phonons of YH_6 taken at different pressure.

III.6. Superconducting characteristics:

The crucial propriety to be defined in this study is the critical temperature where the compound changes the physical state from normal to superconductor phase. The T_c was calculated at different pressures using Allen Dynes and McMillan analytical formulas [13]:

$$T_c = \frac{\theta_D}{1.45} exp\left[\frac{-1.04(1+\lambda)}{\lambda-\mu^*(1+0.62\lambda)}\right] \quad \text{(III.3)}$$

Table III.2 and figure III.6 show the T_c dependence on the pseudo-potential μ^* values at pressure P=150 GPa results indicate the dependence in inverse linear way of the temperature with the pseudo-potential values which is a typical behavior in these compounds.

Table III.2: Critical temperature for different pseudo-potential values at pressure P=150 GPa.

μ*(Ha)	Tc (K°)
0.11	109.43
0.115	107.22
0.12	105.02
0.125	102.82
0.13	100.63
0.136	98.012
0.14	96.27

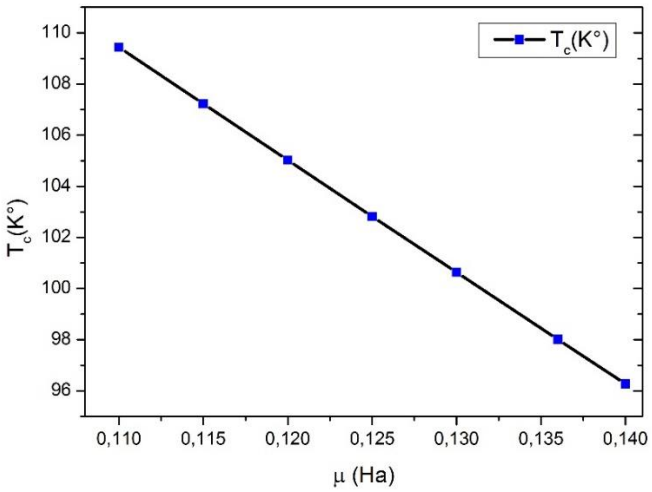

Fig III.6: Variation of the critical temperature as function of pseudo-potential μ*.

Thus, we studied the variation of the critical temperature as a function of pressure P. Table III.3 and figure III.7 summarize the obtained results. We notice that the T_c increases when pressure excesses, until a maximum value of 133 K is recorded at a pressure of 250 GPa, then it begins to decline.We note that the value of pseudo-potential is chosen to be $\mu^* = 0.136$ Ha. By looking at λ values (dimensionless) we can say that the electron-phonon coupling is relatively strong.

Table III.3: Critical temperature and electron-phonon coupling constant at different pressure for μ^*=0.136 Ha.

P(GPa)	Previous studies	This study	
	T_c (K°)	**T_c (K°)**	**λ**
150	-	98.012	1,17191
200	280 [5]	125.276	1,335691
250	300 [5]	133.469	1,36987
300	-	114.98	1,216297

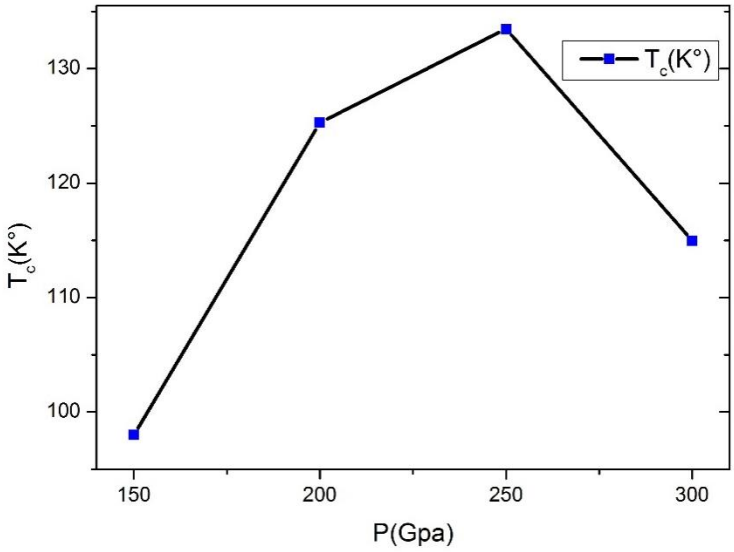

Fig III.7: Variation of the Tc as a function of pressure.

III.6. Superconducting gap

The gap in the density of states at the Fermi level arises from pairing up the conduction electrons. The gap is a common feature of all superconductors. Conventional and unconventional superconductors differ by the pairing mechanism. In conventional superconductors the pairing is due to electron – phonon attractive interaction. Further more, the wave functions corresponding to electron pairs (Cooper pairs), are spatially symmetric like an atomic *s*-orbital with angular momentum L=0. That is to say, the wave function of a pair is unchanged if the positions of the electrons are exchanged. This immediately implies that the spin part of the wave function is anti-symmetric in accordance with the Pauli Exclusion Principle. In particular, the electron pairs are in a spin-singlet state S=0 with anti-parallel spins. The pairing mechanism in a conventional superconductor is thus appropriately called, *s-wave spin-singlet*. The energy gap of an *s*-wave superconductor is finite over the entire Fermi surface. Under ideal circumstances, the magnitude of the gap is the same at all points on the Fermi surface. BCS theory assumes the Fermi surface is spherical (see fig. III.8)

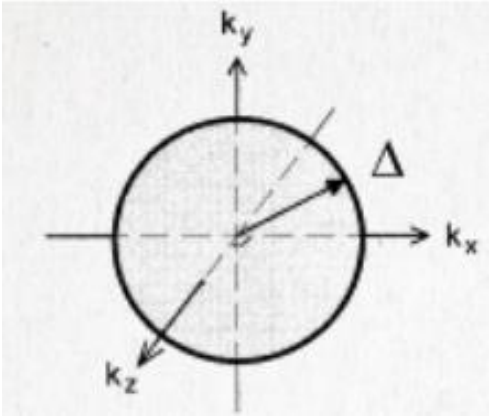

Fig III.8: Picture of an isotropic energy gap for a conventional superconductor in the BCS model.

Superconductors which obey Eq.(I.4) mentioned in chapter I: $\Delta(T) = \Delta_0\left(1-\frac{T}{T_c}\right)^{1/2} = 1.76k_BT_c\left(1-\frac{T}{T_c}\right)^{1/2}$ (are considered to be weakly-coupled, in reference to the weak interaction energy between electrons in a Cooper pair. Some systems produce experimental results which deviate substantially from the BCS results [14]. These materials are more appropriately described by strong-coupling theory where the coupling ratio ($\frac{\Delta_0}{k_BT_c}$) is greater than the BCS prediction of 1.76, which is in our case considering the electron-phonon coupling constant λ values. Despite that, we have tried to calculate and represent this factor characteristic according to the previous study [4]. The obtained results are summarized in table III.4 and Figure III.9.

Table III.4: superconducting gap at different pressure for T=0 K and μ*= 0.136 Ha.

P (GPa)	Δ_0(meV)
150	14,86
200	18,99
250	20,24
300	17,43

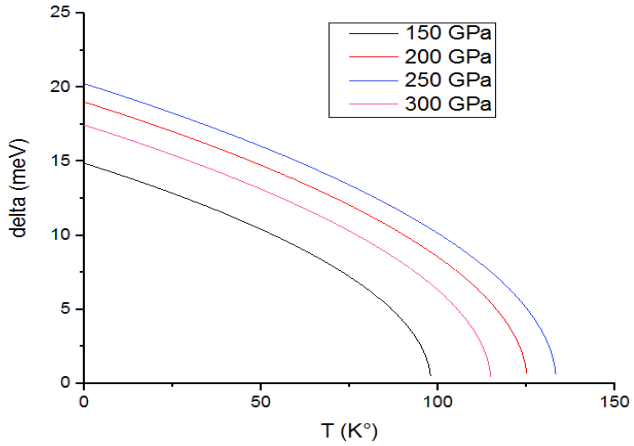

Fig III.9: Isotropic energy gap as a function of temperature at different pressure for μ*= 0.136 Ha.

Our results are so far from that reported in [4] and this is due to the insufficient of the calculation parameters approved as it mentioned previously.

III.7. Coherence length:

In the ground state of the metal the energy levels are filled with two electrons each starting from the lowest level. The highest energy level reached is called the Fermi E_F. At temperature $T \rightarrow 0$ all states below E_F are occupied, all states above E_F are empty. The highest momentum is called the 'Fermi momentum p_F, the highest velocity is the Fermi velocity which can be calculated from the quasi-classical approximation.

$$v_F = \sqrt{\frac{2E_F}{m}} \qquad \text{(III.4)}$$

which is in the order of 10^6 m/s, considering that the material is a non-heavy electron superconductor and the renormalized electron mass m^* is approximately equal to electron mass m ($m \sim m^*$).

Therefore, Pippard [15] introduced the coherence length ζ_0 as a measure of the minimum extent of electronic wave packets.

$$\xi_0 = \frac{2\hbar v_F}{\pi \Delta_0} \qquad \text{(III.5)}$$

We have based on the obtained results of the above section to calculate this characteristic factor (Table III.5)

Table III.5: coherence length at different pressure for T=0 K and μ*= 0.136 Ha.

P (GPa)	$V_F(10^6 m/s)$	ζ_0 (nm)
150	2.335	32,9064541
200	2.43	26,7955537
250	2.51	26,0030044
300	2.58	31,0252324

III.8. Conclusion:

In this chapter, we have study the impact of the pressure on the thermodynamic properties and superconductivity of the YH_6 compound, within DFT and DFPT theories implemented in ABINIT code. Our results look somewhat remote compared to the available data, but they save the general tendencies of these superconductor kinds.

References

[1] P. Hohenberg and W. Kohn, Phys. Rev. B, 136, (1964) 864.

[2] W. Kohn and L.J. Sham, *Phys. Rev. A.***140** (1965) 1133.

[3] P. Giannozzi, S. de Gironcoli, P. Pavone, S. Baroni, *Phys. Rev. B*, **43** (1991) 7231.

[4] Y. Li et al., *nature scientific reports*, **5** (2015) 09948.

[5] G. M. Eliashberg, *JETP***,** *11* (**1959**) 696-702.

[6] K. S. Grishakov, , N. N. Degtyarenko, & E. A. Mazur, *J. Exp. Theor. Phys.* **128** (2019).

[7] C. Heil, S. di Cataldo, G. B. Bachelet, & L. Boeri, *Phys. Rev. B* **99** (2019) 220502

[8] I. A. Troyan1 et al.,

[9] X. Gonze et al., *Kristallogr Z.*,**220** (2005) 558.

[10] J. P. Perdew, K. Burke, M. Ernzerhof, *Phys. Rev. Lett.* **77** (1996) 3865-3868.

[11] H. J. Monkhorst, and J. D. Pack, *Phys. Rev. B.* **8** (1973) 5747.

[12] B. Francis, *Phys. Rev.* **71**(1947) 809-824.

[13] P. B. Allen, R. C. Dynes, *Phys. Rev. B***. 12** *(***1975)** 905-922.

[14] N.W. Ashcroft and N.D. Mermin, "*Solid State Physics"*, Holt, Rinehart and Winston, (1976).

[15] Saint-James, Thomas and Sarma, "*Type-II Superconductivity"*, Pergamon Press Ltd, (1969).

General conclusion

General conclusion

In this thesis, we have study the impact of the pressure on the thermodynamic properties and superconductivity of the YH_6 compound, within DFT and DFPT theories implemented in ABINIT code. We predicted the phonons behavior under various pressures and we calculated the critical temperature using McMillan formula, superconducting gap and coherence length. We showed that:

- The phonon spectrums exhibit positive frequencies at different pressures (150, 200, 250 and 300 Gpa), which indicates that YH_6 compound with space group $Im\bar{3}m$ is dynamically stable at these hydrostatic pressures.
- The critical temperatures calculated are: 98.012, 125.276, 133.469 and 114.98 K° at the pressures mentioned previously. Those values make this compound a superconductor material with a high Tc.
- Thus, the coherence lengths calculated are: 32, 90, 26, 79, 26, 01 and 31, 02 nm at the same pressure conditions.

Our results look somewhat remote compared to the available data, but they save the general tendencies of these superconductor kinds.

We hope to pursuit this study by extending the predictions s to the other properties and materials with suffisent calculation parameters.

People's Democratic Republic of Algeria

Ministry of Higher Education
& Scientific Research
University Mohamed Khider, Biskra

RSDT

Faculty of Exact Sciences
& Nature Sciences & Life Sciences
Department of Matter Sciences

Certificate

The president of the organizing committee certifies that

CHERIET Abderrahmane

With a **Poster** communication entitled:

Theoretical study of the structural and electronic properties of Cesium-Thallium halide Perovskite materials

Attended the

13JCTC (13th International Days of Theoretical and Computational Chemistry)

Held on February 02nd and 03rd, 2020 at the University of Biskra, Algeria

Co-authors: B. Lagoun, A. Alhussein, A. Chadli, M. Halit, M. Zaabat, A. Labed and A. Begagra

Pr. BOUTARFAIA Ahmed
Rector of University of Biskra

الملخص

الهدف من هذا العمل هو حساب الخصائص البنيوية و الإهتزازية، بالإضافة إلى درجة الحرارة الحرجة، طاقة الفجوة فائقة التوصيل و طول رابطة ثنائية كوبر لمركب YH_6و الذي يعتبر واحد من الموصلات الفائقة الجديدة يسمى هيدريد اليتيريوم ذو بنية مكعبة و التي تظهر عند ضغوط عالية. تم إجراء الحسابات باستعمال ABINIT اعتمادا على نظرية الكثافة الوظيفية (DFT) و نظرية اضطراب الكثافة الوظيفية (DFPT)،حيث يتميز بدرجة حرارة مرتفعة عند ضغط عالي و هذا ما لاحظناه في النتائج المتحصل عليها، رغم أن نتائجنا تبدو بعيدة بعض الشيء عن البيانات المتاحة إلا أننا لم نخرج عن إطار الميول العامة لهذا النوع من الموصلات الفائقة.

الكلمات المفتاحية: الخصائص البنيوية، الخصائص الإهتزازية، ، درجة الحرارة الحرجة ، طاقة الفجوة فائقة التوصيل، طول رابطة ثنائية كوبر، موصلات فائقة،، هيدريد اليتيريوم، بنية مكعبة، ،ABINIT،DFT،DFPT.

Abstract

The objective of this work is calculation of the structural, andVibrational properties in addition to critical temperature, superconducting gap, and coherence length of cooper pairs of YH_6 which is one of the new superconductors called Clathrate Yttrium hydride which has cubic structure that appears at high pressures. The calculation was conducted using ABINIT code in the framework of the functional theory of density (DFT), and the density functional perturbation theory (DFPT), It is characterized by high temperature at high pressure and this is what we have observed in the results obtained, although our results seem to be somewhat distant from the available data, we are not out of the general trend frame of this type of superconductors.

Key words: structural properties, Vibrational properties, critical temperature, superconducting gap, coherence length of cooper pair, superconductors, Clathrate Yttrium hydride, cubic structure, ABINIT, DFT, DFPT.

Résumé

L'objectif de ce travail est de calculer des propriétés structurelle et vibratoire en plus de température critique, le gap supraconducteur et la longueur de cohérence de pair de Cooper de YH_6, qui est l'un des nouveaux supraconducteurs appelé hydrure de Yttrium de structure cubique à haute pression. Le calcul a été réalisé en utilisant le logiciel ABINIT dans le cadre de la théorie fonctionnelle de la densité (DFT), la théorie de perturbation de densité fonctionnelle (DFPT).Il est caractérisé par une température élevée à haute pression et c'est ce que nous avons observé dans les résultats obtenus, bien que nos résultats semblent être quelque peu éloignés des données disponibles, nous ne sommes pas en dehors de la tendance générale de ce type de supraconducteurs.

Mots clés : propriétés structurelles, propriétés vibratoires, température critique, gap supraconducteur, longueur de cohérence de la paire de cuivre, supraconducteurs, hydrure Yttrium, structure cubique, DFT, ABINIT, DFPT.